IEEE Access
Multidisciplinary ⋮ Rapid Review ⋮ Open Access Journal

Received December 25, 2019, accepted January 9, 2020, date of publication January 13, 2020, date of current version January 30, 2020.

Digital Object Identifier 10.1109/ACCESS.2020.2966281

Co-Design of Dual Security Control and Communication for Nonlinear CPS Under DoS Attack

LI ZHAO [1,2] AND WEI LI [1,3,4]
[1]College of Electrical and Information Engineering, Lanzhou University of Technology, Lanzhou 730050, China
[2]College of Electrical Engineering, Longdong University, Qingyang 745000, China
[3]Key Laboratory of Gansu Advanced Control for Industrial Processes, Lanzhou University of Technology, Lanzhou 730050, China
[4]National Demonstration Center for Experimental Electrical and Control Engineering Education, Lanzhou University of Technology, Lanzhou 730050, China

Corresponding author: Wei Li (liwei@lut.cn)

This work was supported in part by the National Natural Science of China under Grant 61364011 and Grant 61763027, and in part by the Higher Education Innovation Capacity Improvement Project of Gansu in China under Grant 2019B-152.

ABSTRACT The less conservative co-design problem of dual security control and communication for CPS was studied for a class of nonlinear CPS with an actuator fault and DoS attack based on the DETCS. First, combining with the edge computing thought, data filtering and partial computing tasks were assigned to the network edge devices. The DoS attack with limited energy is converted into a special time delay; thus, the discrete event trigger condition, the actuator fault estimation and regulation, and the robustness for DoS attack can be considered uniformly. A dual security control framework of non-uniformly sampled data system was proposed under the DETCS for CPS, and the T-S fuzzy model of closed-loop nonlinear CPS with the co-existence of fault and attack was established. Second, with the help of time-delay system theory, a robust observer for state and fault estimation and the co-design method of dual security control and communication with the actuator fault and DoS attack were obtained by constructing an appropriate Lyapunov-Krasovskii function and using affine Bessel-Legendre inequality. Finally, the validity and feasibility of the theoretical results were verified by a classical quadruple-tank system.

INDEX TERMS Co-design, DoS attack, dual security control, nonlinear CPS.

I. INTRODUCTION

Cyber-physical systems (CPSs) integrate the 3C technology of computer, communication and control, which is an intelligent system with highly integrated interaction between computing units and physical objects in the network environment [1]. Its emergence has promoted the rapid development of the aerospace, smart cities, smart grids, intelligent transportation and other fields. Furthermore, CPS realizes the information interaction for physical subsystems through various shared communication networks, so the cyber system and the physical system are deeply integrated. However, the diversified communication network in CPSs makes the system more vulnerable to external influences, including cyber-attack, malicious code, data fraud, network eavesdropping and so on, which pose a serious threat to the security of the cyber system. In addition, physical system fault is another aspect that affects CPS security, and the physical system in CPSs have changed from closed and isolated to open and interconnected. Therefore, CPSs should not only ensure the security of the physical systems, but also maintain the network security of the cyber systems, and the two are mutually coupled and deeply related to guarantee the integrity of CPSs [2], [3].

The safe operation of various physical components in a CPS is the basis for ensuring the stability of the system. If the erosion of network insecurity factors is put aside, the fault of physical components is one of the serious threats to the system security. Fortunately, fault-tolerant control theory provides an effective way to deal with the fault problem of components in CPS. Over the past two decades, fault-tolerant control has made progress from three aspects: passive fault tolerance [4]–[6], active fault tolerance [7]–[10] and hybrid fault tolerance [11]–[13]. However, the above results are only a single consideration for physical system security under component faults; the security of the cyber system under the

The associate editor coordinating the review of this manuscript and approving it for publication was Juntao Fei.

cyber-attack is not involved. While the CPS is a community of the physical system and the cyber system, both are indispensable. As a result, only considering the dual security defence system of fault tolerance in the physical system and attack tolerance in the cyber system can the CPS security be ensured [14], [15]. In addition, most of the plants are nonlinear in practical engineering. Therefore, it is significant to study the dual security control of fault tolerance and attack tolerance for nonlinear CPSs. This is the first motivation for the research.

Recently, CPS security incidents have occurred frequently. The most representative events include: the Stuxnet Worm attacked Iranian nuclear facilities and caused nuclear power plant to shut down [16], [17], the Havex Trojans assaulted European industrial manufacturing systems and led to hydroelectric dams being out of control [18], and the BlackEnergy3 destroyed the Ukrainian power grid and resulted in 220,000 people losing their power supply [19]. The commonalities of the above incidents are cyber-physical coupling and attack concealment. Among more than ten kinds of attacks summarized in the existing literature, denial of service attacks (DoS), false data injection attacks and data replay attacks are hot topics. Liu *et al.* [20] classified CPS attacks into four categories from the perspective of spatial concealment and temporal concealment: space concealed attacks, time concealed attacks, space-time concealed attacks, and non-concealed attacks. Obviously, the DoS attack is a non-covert attack that blocks the communication channel and makes system communication unable to carry on normally. The attack on Ukraine's power grid happened to use the DoS attack to block communication. Additionally, DoS attack requires neither prior knowledge of the system nor read-write permission to control and measure signals, so it is easy to implement on the system. However, the defender has no good method to eliminate it, and many scholars try to find good solutions [21]–[25]. Hu *et al.* [23] designed a new periodic resilient event-triggering communication scheme and constructed a new state error-dependent switched system model, and achieved the desired stability of the switched system under the known periodic DoS jamming attacks. Wang and Xu [24] established an attack tolerance mechanism and designed a guaranteed performance controller to ensure the exponential mean square stability of CPS under DoS attack. Su and Ye [25] established an attack compensation mechanism and proposed a new DoS attack detection strategy based on packet acceptance rate, as well as studying the co-design problem of DoS attack detection and compensation. However, all of the above researches did not involve component faults in CPS. Therefore, it is necessary to establish a dual security defence system with DoS attack and physical component fault for CPS. This is the second motivation for this paper.

High-efficiency means that the system achieves satisfactory performance while consuming as little resources as possible. However, there are two obvious problems for CPS efficiency. First, the large amount of perception information in the CPS leads to the explosive growth of data transmission. If only relying on the traditional control centre to process massive data, it will certainly increase the computing burden and communication load. Second, many agents in CPS do not fully utilize their computing efficiency, and not all the massive data for control need to be transmitted by the limited bandwidth network. For the above problems, the following two strategies can solve them. First, the rise of edge computing [26], [27] makes the task of data processing no longer rely solely on the control centre; instead, the task can be partially migrated to other network edge devices as needed, which reduce the burden on the control centre. Second, in order to reduce the transmission of redundant data, effectively save network resource, and realize the co-design between communication and control, the discrete event-triggered communication scheme (DETCS) [28]–[30] was put forward to filter the transmitted data according to the system requirements. So, the organic combination of the two aspects will provide strong support for realizing high-efficiency. Lu and Yang [31] designed a discrete security observer to estimate the state and attack when the double-end network was subject to adversarial attack, and achieved the co-design of the observer and the controller; however, the co-application of the edge computing concept and the DETCS was not involved. Therefore, in order to realize high-efficiency, some computing tasks are allocated to network edge devices with the help of the edge computing concept, and the task of data filtering and processing are completed by edge devices based on DETCS. This is the third motivation of this paper.

Based on the above analysis, the co-design method of communication and dual security control of fault tolerance and attack tolerance was studied for nonlinear CPSs with an actuator fault and DoS attack. The main contributions are summarized as follows.

1) With the help of the edge computing concept, different computing tasks were assigned to the network edge equipment and the control centre according to the system requirements, and the system states, fault estimation and the transmitted data filtering were no longer completed by the control centre, but were transferred to the network edge equipment, so as to save network resources and improve computing efficiency.

2) Under DETCS, the malicious packet loss caused by DoS attack with limited energy was converted into a special delay. The non-uniformly sampled data system framework for CPS under DoS attack was proposed, and the closed-loop model of the nonlinear CPS was established that integrates actuator fault, DoS attack and discrete event trigger conditions.

3) For the problems of estimation and security control, under the framework of unified sampled data system, the appropriate Lyapunov-Krasovskii function was constructed, with the help of the time-delay system theory and the affine Bessel-Legendre inequality, the robust observer of the state and fault estimate and the controller of fault-tolerant actively and attack-tolerant passively

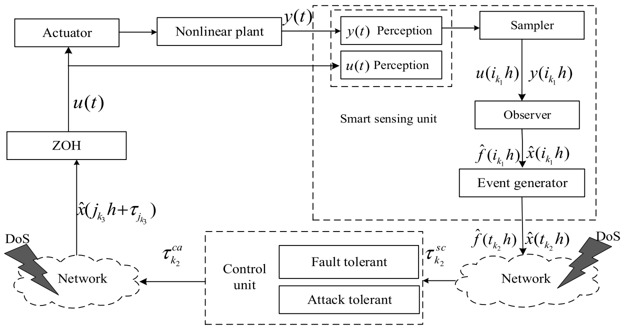

FIGURE 1. Scheme diagram of CPS dual security control.

are obtained. Thus, the co-design of dual security and saving network communication resources was achieved.

The rest of the paper is organized as follows. Section 2 presents a description of the system. Sections 3 and 4 develop an observer with robust H_∞ state and fault estimation and co-design of dual security control and communication. A quadruple-tank simulation experiment is presented in Section 5. Section 6 concludes this paper.

Notation: $\boldsymbol{R}^n$ and $\boldsymbol{R}^{m\times n}$ denote the n-dimensional Euclidean space and the set of all $m \times n$ real matrices, respectively. $\boldsymbol{A} > \mathbf{0}$ and $\boldsymbol{A} < \mathbf{0}$ represent positive and negative definiteness, respectively, and $\boldsymbol{A}^T$ denotes the transpose of matrix $\boldsymbol{A}$. The notation $\|\cdot\|$ stands for the 2-norm. In symmetric block matrices, the notation $*$ is used to indicate a term that is induced by symmetry. $\lambda_{\max}(\boldsymbol{A})$ and $\lambda_{\min}(\boldsymbol{A})$ denote the maximum and minimum eigenvalues of matrix $\boldsymbol{A}$, respectively, and $diag\{\cdots\}$ represents the block-diagonal matrix.

II. SYSTEM DESCRIPTION

A. SYSTEM FRAMEWORK

Considering a class of nonlinear CPSs with actuator fault and DoS attack on the double-end networks of the sensor-controller and controller-actuator, based on edge computing thought and DETCS, the CPS dual security control framework was established as shown in Figure 1.

The system includes the nonlinear controlled object, smart sensing unit, control unit, zero-order hold (ZOH), actuator and double-end networks. Among them, the smart sensing unit, namely the network edge equipment, including the perception of $y(t)$ and $u(t)$, the sampler, the observer and the event generator, can estimate the system state and fault in real time while detecting the system output, and the filtering of the transmitted data are performed by the event generator. The control unit contains a controller with the fault-tolerant and attack-tolerant ability to meet the security requirements for the system. In addition, the double-end networks are affected by DoS attack that block or delay network communication to make information interrupted or unavailable.

Assumption 1: The energy of DoS attack is limited; that is, the duration of DoS attack is finite when it occurs. If the impact of DoS attack on the system is regarded as a special kind of packet loss, then the amount of packet loss is also limited.

Assumption 2: After the event generator is introduced into the smart sensor unit of the network edge device, through the co-design of control and communication, the natural packet loss in the network transmission has rarely occurred.

Assumption 3: The sampler is clock-driven with equal period h and corresponding sampling sequence is $\{i_{k_1}\}$, $k_1 = 0, 1, 2, \cdots$. Both the controller and actuator are event-driven. The trigger period that sends data after being filtered by the event generator is recorded as $h_{t_{k_2}}$, $h_{t_{k_2}} = \left(t_{k_2+1} - t_{k_2}\right)h$, and the send sequence is $\{t_{k_2}\}$, $k_2 = 0, 1, 2, \cdots$. Once affected by DoS attack, the transmission period of the successfully transmitted data after filtering is $h_{j_{k_3}}$, $h_{j_{k_3}} = \left(j_{k_3+1} - j_{k_3}\right)h$, the transmission sequence is $\{j_{k_3}\}$. The above data sequence interval is satisfied if $t_{k_2} = mi_{k_1}$, $j_{k_3} = ni_{k_1}$, m, n are integers.

B. DESCRIPTION OF THE CONTROLLED PLANT MODEL

Considering a class of nonlinear controlled plants by using the CPS security control framework in the above, since the controlled plant is continuous, while both the smart sensing unit and control unit are the digital value of the estimation and calculation, so the system is a typical data sampling system, which is shown in Figure 1.

$$\begin{cases}\dot{x}(t) = \boldsymbol{F}(x(t), u(t), f(t), w(t)) \\ \qquad = f(x(t)) + g(x(t))(u(t), f(t), w(t)) \\ y(i_{k_1}) = \boldsymbol{C}(x(i_{k_1}), v(i_{k_1}))\end{cases} \tag{1}$$

where $x(t) \in \boldsymbol{R}^n$ and $u(t) \in \boldsymbol{R}^{n_u}$ are system state and control inputs. $f(t) \in \boldsymbol{R}^{n_f}$ is the unknown continuous time-varying actuator fault and its derivative norm is assumed to be bounded; that is, there is a constant f_1 such that $\left\|\dot{f}(t)\right\| \leq f_1$. $w(t) \in \boldsymbol{R}^{n_w}$, $y(i_{k_1}) \in \boldsymbol{R}^m$ and $v(i_{k_1}h) \in \boldsymbol{R}^{n_v}$ are system disturbance, the sampled output and measurement noise, respectively. $\{i_1, i_2, \cdots, i_{k_1}, \cdots\}$ represents the sampling time of the sampler in the system. $f(x(t))$, $g(x(t))$ and $\boldsymbol{C}(x(t))$ are dependent on an unknown nonlinear function $x(t)$.

Using the nonlinear T-S fuzzy modelling method, the following fuzzy system state equation can be obtained:

$$\begin{cases}\dot{x}(t) = \sum\limits_{i=1}^{r} \xi_i(\theta(t))[\boldsymbol{A}_i x(t) + \boldsymbol{B}_i u(t) + \boldsymbol{E}_{fi} f(t) + \boldsymbol{E}_{wi} w(t)] \\ y(i_{k_1}) = \sum\limits_{i=1}^{r} \xi_i(\theta(t))[\boldsymbol{C}_i x(i_{k_1}) + \boldsymbol{E}_{vi} v(i_{k_1})]\end{cases} \tag{2}$$

where $\xi_i(\theta(t)) = a_i(\theta(t)) \Big/ \sum\limits_{i=1}^{N} a_i(\theta(t))$, $\xi_i(\theta(t))$ is the weight ratio of each fuzzy rule, $a_i(\theta(t)) = \prod\limits_{j=1}^{N} \boldsymbol{M}_{ij}(\theta_j(t))$ and $\boldsymbol{M}_{ij}(\theta_j(t))$ is a membership function of $\theta_j(t)$ with respect to $\boldsymbol{M}_{ij}$. Suppose that $a_i(\theta(t)) \geq 0 (i = 1, 2, \cdots, N)$ and $\sum\limits_{i=1}^{N} a_i(\theta(t)) > 0$, then $\xi_i(\theta(t)) \geq 0$ and $\sum\limits_{i=1}^{N} \xi_i(\theta(t)) = 1$, $\boldsymbol{A}_i, \boldsymbol{B}_i, \boldsymbol{E}_{fi}, \boldsymbol{E}_{wi}, \boldsymbol{C}_i, \boldsymbol{E}_{vi}$ are known matrices with the appropriate dimensions.

C. DISCRETE EVENT TRIGGER COMMUNICATION SCHEME

According to the analysis in the above, the event generator in the smart sensing unit is mainly used for data filtering, so the following typical discrete triggering conditions are adopted in [29].

$$e^T(i_{k_1}h)\mathbf{\Phi} e(i_{k_1}h) \leq \sigma_s \hat{x}^T(t_{k_2}h)\mathbf{\Phi}\hat{x}(t_{k_2}h) \tag{3}$$

where $\sigma_s \in [0, 1)$ is a predefined event trigger parameter and related to the expected performance of the system, $\mathbf{\Phi}$ is the positive definite symmetric matrix to be designed, $\hat{x}(i_{k_1}h) - \hat{x}(t_{k_2}h) = e(i_{k_1}h)$ is the state estimation error, $\hat{x}(i_{k_1}h)$ represents the most recent system state value estimated by the observer and $\hat{x}(t_{k_2}h)$ denotes the latest system state estimate value that was filtered by the event generator at the last moment and will be transmitted to the control unit.

D. ANALYSIS OF THE CORRELATION TIME DELAY INTERVAL OF CPS

From the CPS dual security control framework, the data at the output end of the continuous system is sampled in equal period, and the introduction of the event generator and the occurrence of DoS attack make the filtered data transmit to the control unit in a non-uniform manner.

For a class of data sampling system represented by Equation (2), three methods are stated in Xiao *et al.* [32] to research it, among them, the preferred method is to transform the influence of uniform or non-uniform sampling period on system attributes into the impact of time delay on the system through the time-delay theory in [33], and then to design corresponding observer and controller in a continuous manner. Therefore, the correlation time delay interval of the state and fault estimation and the CPS dual security control part will be defined and analysed as follows.

1) A TIME DELAY ANALYSIS OF STATE AND FAULT ESTIMATION IN AN EDGE SMART SENSING UNIT FOR CPS

In the smart sensing unit of the edge equipment, the system output is sampled at equal period. Considering that the impact of fault on the system need to be found in time, then the output data is obtained directly to estimate the state and fault in an equal period. The controlled plant is continuous, and the input data of the observer is discrete, so the sampling period is converted into a time delay between two adjacent sampling points. On this basis, the design and analysis of the state and fault observer are carried out.

Define the time delay function:

$$\tau_1(t) = t - i_{k_1}h \tag{4}$$

where, $t \in [i_{k_1}h, i_{k_1+1}h)$ and $0 \leq \tau_1(t) \leq h_1 = h$.

2) TIME DELAY ANALYSIS OF CONTROL VARIABLES IN THE CONTROL UNIT

In order to more clearly describe the process of the data sampling, filtering and transmitting under DoS attack, the corresponding sequence diagram is shown in Figure 2.

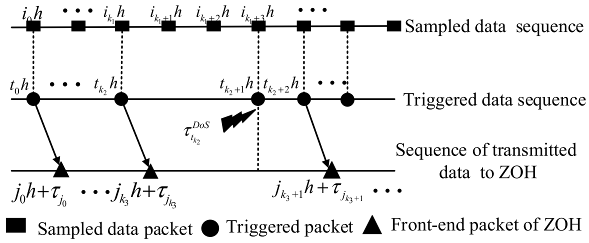

FIGURE 2. Schematic diagram of CPS non-uniform transmission data update under a DoS attack.

In Figure 2, $\tau_{t_{k_2}}^{DoS}$ is the number of consecutive packet loss caused by DoS attack on the controller of the double-end networks, and the duration of DoS attack is $\tau_{DoS} \leq \tau_M^{DoS} h_{t_{k_2}}^{\max}$. Where, τ_M^{DoS} is the maximum number of consecutive packet loss, $h_{t_{k_2}}^{\max}$ is the maximum non-uniform triggering period of data filtered by event generator, $i_{k_1}h$ is the sampling data sequence of the sampler, $t_{k_2}h$ is the triggered data sequence after data filtering by event generator and $j_{k_3}h$ is the sequence of transmitted data to the ZOH side after the DoS attack on the double-end network without considering time delay, $j_{k_3}h = t_{k_2}h + \tau_{t_{k_2}}^{DoS} h_{t_{k_2}}$. The network transmission delay of the data successfully transmitted to the ZOH side is $\tau_{j_{k_3}}$, and $\tau_{j_{k_3}} = \tau_{j_{k_3}}^{sc} + \tau_{j_{k_3}}^{c} + \tau_{j_{k_3}}^{ca}$, where, $\tau_{j_{k_3}}^{sc}$ is sensor-controller network delay, $\tau_{j_{k_3}}^{c}$ is the calculation delay, and $\tau_{j_{k_3}}^{ca}$ is the controller-actuator network delay. In the practical system, the network transmission delay $\tau_{j_{k_3}}$ is much smaller than the sampling and transmission period and can be ignored.

Considering the network delay, when $\hat{x}(j_{k_3}h)$ and $\hat{f}(j_{k_3}h)$ are transmitted to the front end of the ZOH, while $\hat{x}(j_{k_3+1}h)$ and $\hat{f}(j_{k_3+1}h)$ are not sent to the ZOH, then the following transmission interval is defined: $\Lambda = \left[j_{k_3}h + \tau_{j_{k_3}}, j_{k_3+1}h + \tau_{j_{k_3+1}}\right)$.

Define the time delay function:

$$\tau_2(t) = t - j_{k_3}h \tag{5}$$

Its upper and lower bounds are respectively as follows: $\max\left\{h_{t_{k_2}} + \tau_{t_{k_2}}^{DoS} h_{t_{k_2}} + \tau_{j_{k_3}}\right\} \leq h_{t_{k_2}}^{\max} + \tau_M^{DoS} h_{t_{k_2}}^{\max} + \tau_{j_{k_3}}^{\max} = h_2, 0 < \tau_{\min} = \min\left\{\tau_{t_{k_2}}^{DoS} h_{t_{k_2}} + \tau_{j_{k_3}}\right\} = \tau_{j_{k_3}}^{\min}$. Where, $\tau_{j_{k_3}}^{\max}$, $\tau_{j_{k_3}}^{\min}$ are upper and lower bounds of network transmission delay. Then, the delay function satisfies $0 < \tau_{\min} \leq \tau_2(t) \leq h_2$. For convenience, $i_{k_1}h$, $t_{k_2}h$ and $j_{k_3}h$ will be denoted as i_{k_1}, t_{k_2} and j_{k_3} in the following analysis.

III. DESIGN OF ROBUST H_∞ STATE AND FAULT ESTIMATION OBSERVER UNDER DoS ATTACK

In a sampling period, the sampling characteristic of CPS on the output side are analysed by using the time delay method. The discrete sampling output equation is kept at zero-order in [34] and the following continuous time-varying time delay output can be obtained:

$$y(t) = \sum_{i=1}^{r} \xi_i(\theta(t))[\boldsymbol{C}_i x(t - \tau_1(t)) + \boldsymbol{E}_{vi} v(t - \tau_1(t))] \tag{6}$$

The generalized observer for state and fault estimation is constructed as follows:

$$\begin{cases}\dot{\hat{x}}(t)=\sum\limits_{i=1}^{r}\sum\limits_{j=1}^{r}\xi_i(\theta(t))\xi_j(\theta(t))[\boldsymbol{A}_i\hat{x}(t)+\boldsymbol{B}_iu(t)\\ \qquad +\boldsymbol{E}_{fi}\hat{f}(t)-\boldsymbol{L}_j(\hat{y}(t)-y(t))]\\ \hat{y}(t)=\sum\limits_{i=1}^{r}\xi_i(\theta(t))[\boldsymbol{C}_i\hat{x}(t-\tau_1(t))]\\ \dot{\hat{f}}(t)=\sum\limits_{j=1}^{r}\xi_j(\theta(t))[-\boldsymbol{F}_je_y(t)]\end{cases} \tag{7}$$

where $\hat{x}(t)\in\boldsymbol{R}^n$ is the state estimation value, $\hat{y}(t)\in\boldsymbol{R}^m$ is the observer output value, $\hat{f}(t)$ is a fault estimation value, $\boldsymbol{L}_j$ and $\boldsymbol{F}_j$ are the observer gain matrix and fault estimation gain matrix, respectively.

Define $e_x(t)=\hat{x}(t)-x(t)$, $e_y(t)=\hat{y}(t)-y(t)$ and $e_f(t)=\hat{f}(t)-f(t)$, the following error system can be obtained:

$$\begin{cases}\dot{e}_x(t)=\dot{\hat{x}}(t)-\dot{x}(t)=\sum\limits_{i=1}^{r}\sum\limits_{j=1}^{r}\xi_i(\theta(t))\xi_j(\theta(t))[\boldsymbol{A}_ie_x(t)\\ \qquad +\boldsymbol{E}_{fi}e_f(t)-\boldsymbol{L}_j\boldsymbol{C}_ie_x(i_{k_1})+\boldsymbol{L}_j\boldsymbol{E}_{vi}(i_{k_1})-\boldsymbol{E}_{wi}w(t)]\\ e_y(t)=\sum\limits_{i=1}^{r}\xi_i(\theta(t))[\boldsymbol{C}_ie_x(i_{k_1})-\boldsymbol{E}_{vi}v(i_{k_1})]\end{cases} \tag{8}$$

The derivative of fault estimation error with respect to time is:

$$\dot{e}_f(t)=-\dot{f}(t)+\sum_{i=1}^{r}\sum_{j=1}^{r}\xi_i(\theta(t))\xi_j(\theta(t))[\boldsymbol{F}_j\boldsymbol{E}_{vi}v(i_{k_1}) -\boldsymbol{F}_j\boldsymbol{C}_ie_x(i_{k_1})] \tag{9}$$

Define $\bar{\boldsymbol{A}}_i=\begin{bmatrix}\boldsymbol{A}_i & \boldsymbol{E}_{fi}\\ \boldsymbol{0} & \boldsymbol{0}\end{bmatrix}$, $\bar{e}(t)=\begin{bmatrix}e_x(t)\\ e_f(t)\end{bmatrix}$, $\bar{\boldsymbol{C}}_i=\begin{bmatrix}\boldsymbol{C}_i & \boldsymbol{0}\end{bmatrix}$, $\bar{\boldsymbol{L}}_j=\begin{bmatrix}\boldsymbol{L}_j\\ \boldsymbol{F}_j\end{bmatrix}$, $\bar{\boldsymbol{E}}_{wi}=\begin{bmatrix}\boldsymbol{E}_{wi} & \boldsymbol{0}\\ \boldsymbol{0} & \boldsymbol{I}\end{bmatrix}$ and $\bar{w}(t)=\begin{bmatrix}w(t)\\ \dot{f}(t)\end{bmatrix}$.

Then, the augmented error system is:

$$\dot{\bar{e}}(t)=\sum_{i=1}^{r}\sum_{j=1}^{r}\xi_i(\theta(t))\xi_j(\theta(t))[\bar{\boldsymbol{A}}_i\bar{e}(t)-\bar{\boldsymbol{L}}_j\bar{\boldsymbol{C}}_i\bar{e}(t-\tau_1(t)) -\bar{\boldsymbol{E}}_{wi}\bar{w}(t)+\bar{\boldsymbol{L}}_j\boldsymbol{E}_{vi}v(t-\tau_1(t))] \tag{10}$$

Theorem 1: For the error system in Eq.(10), which is augmented by a class of nonlinear CPS with actuator fault and DoS attack in Eq. (2), state and fault estimation observer in Eq. (7) and the derivative of fault estimation error in Eq. (9), for given parameters $h_1>0$ and $\gamma_1>0$, if there exist symmetric matrix $\boldsymbol{P}>\boldsymbol{0}$ and the appropriate dimension matrix $\boldsymbol{X}$, $\boldsymbol{Y}_j$, and making the following inequalities hold:

$$\begin{bmatrix}\boldsymbol{I}_{11} & \boldsymbol{I}_{12} & \boldsymbol{I}_{13} & \boldsymbol{I}_{14} & \boldsymbol{0}\\ * & \boldsymbol{I}_{22} & \boldsymbol{I}_{23} & \boldsymbol{I}_{24} & h_1n_1\bar{\boldsymbol{C}}_i^T\boldsymbol{Y}_j^T\\ * & * & \boldsymbol{I}_{33} & \boldsymbol{I}_{34} & \boldsymbol{0}\\ * & * & * & \boldsymbol{I}_{44} & \boldsymbol{0}\\ * & * & * & * & -h_1n_1\boldsymbol{P}\end{bmatrix}<\boldsymbol{0} \tag{11}$$

$$\begin{bmatrix}\boldsymbol{I}'_{11} & \boldsymbol{I}'_{12} & \boldsymbol{I}_{13} & \boldsymbol{I}_{14} & \boldsymbol{X}\\ * & \boldsymbol{I}'_{22} & \boldsymbol{I}_{23} & \boldsymbol{I}_{24} & \boldsymbol{X}\\ * & * & \boldsymbol{I}_{33} & \boldsymbol{I}_{34} & \boldsymbol{X}\\ * & * & * & \boldsymbol{I}_{44} & \boldsymbol{X}\\ * & * & * & * & -\dfrac{15n_1}{23h_1}\boldsymbol{P}\end{bmatrix}<\boldsymbol{0} \tag{12}$$

$$\begin{bmatrix}\boldsymbol{\Pi}_{11} & \boldsymbol{\Pi}_{12} & \boldsymbol{\Pi}_{13} & \boldsymbol{\Pi}_{14} & \boldsymbol{\Pi}_{15} & \boldsymbol{\Pi}_{16} & \boldsymbol{0}\\ * & \boldsymbol{\Pi}_{22} & \boldsymbol{\Pi}_{23} & \boldsymbol{\Pi}_{24} & \boldsymbol{\Pi}_{25} & \boldsymbol{\Pi}_{26} & \boldsymbol{\Pi}_{27}\\ * & * & \boldsymbol{\Pi}_{33} & \boldsymbol{\Pi}_{34} & \boldsymbol{0} & \boldsymbol{0} & \boldsymbol{0}\\ * & * & * & \boldsymbol{\Pi}_{44} & \boldsymbol{0} & \boldsymbol{0} & \boldsymbol{0}\\ * & * & * & * & \boldsymbol{\Pi}_{55} & \boldsymbol{\Pi}_{56} & \boldsymbol{\Pi}_{57}\\ * & * & * & * & * & \boldsymbol{\Pi}_{66} & \boldsymbol{0}\\ * & * & * & * & * & * & \boldsymbol{\Pi}_{77}\end{bmatrix}<\boldsymbol{0} \tag{13}$$

$$\begin{bmatrix}\boldsymbol{\Pi}'_{11} & \boldsymbol{\Pi}'_{12} & \boldsymbol{\Pi}'_{13} & \boldsymbol{\Pi}'_{14} & \boldsymbol{\Pi}'_{15} & \boldsymbol{\Pi}'_{16} & \boldsymbol{X}\\ * & \boldsymbol{\Pi}'_{22} & \boldsymbol{\Pi}'_{23} & \boldsymbol{\Pi}'_{24} & \boldsymbol{0} & \boldsymbol{0} & \boldsymbol{X}\\ * & * & \boldsymbol{\Pi}'_{33} & \boldsymbol{\Pi}'_{34} & \boldsymbol{0} & \boldsymbol{0} & \boldsymbol{X}\\ * & * & * & \boldsymbol{\Pi}'_{44} & \boldsymbol{0} & \boldsymbol{0} & \boldsymbol{X}\\ * & * & * & * & \boldsymbol{\Pi}'_{55} & \boldsymbol{0} & \boldsymbol{0}\\ * & * & * & * & * & \boldsymbol{\Pi}'_{66} & \boldsymbol{0}\\ * & * & * & * & * & * & \boldsymbol{\Pi}'_{77}\end{bmatrix}<\boldsymbol{0} \tag{14}$$

Then, the state observer gain matrix $\boldsymbol{L}_j$ and fault estimation gain matrix $\boldsymbol{F}_j$ with attack tolerance can be obtained from $\bar{\boldsymbol{L}}_j=\begin{bmatrix}\boldsymbol{L}_j\\ \boldsymbol{F}_j\end{bmatrix}$, and the error system in Eq. (10) is asymptotically stable and meets the following performance indexes:

$$\|\ \bar{e}(t)\ \|_2^2\leq\gamma_1^2\left[\|\ \bar{w}(t)\ \|_2^2+\sum_{k=0}^{+\infty}\left(i_{k_1+1}-i_{k_1}\right)\|\ v(i_{k_1})\ \|_2^2\right].$$

where

$$\begin{aligned}\boldsymbol{I}_{11}&=\boldsymbol{P}\bar{\boldsymbol{A}}_i+\bar{\boldsymbol{A}}_i^T\boldsymbol{P}-n_2\boldsymbol{P}+n_3\boldsymbol{P}-3\boldsymbol{X}-3\boldsymbol{X}^T+h_1n_1\bar{\boldsymbol{A}}_i^T\boldsymbol{P}\bar{\boldsymbol{A}}_i\\ &\quad+h_1n_2\left(\boldsymbol{P}\bar{\boldsymbol{A}}_i+\bar{\boldsymbol{A}}_i^T\boldsymbol{P}\right)\\ \boldsymbol{I}_{12}&=-\boldsymbol{Y}_j\bar{\boldsymbol{C}}_i+n_2\boldsymbol{P}+\boldsymbol{X}-3\boldsymbol{X}^T-h_1n_1\bar{\boldsymbol{A}}_i^T\boldsymbol{Y}_j\bar{\boldsymbol{C}}_i-h_1n_2\boldsymbol{Y}_j\bar{\boldsymbol{C}}_i\\ &\quad-h_1n_2\bar{\boldsymbol{A}}_i^T\boldsymbol{P}\\ \boldsymbol{I}_{13}&=2\boldsymbol{X}-3\boldsymbol{X}^T,\quad \boldsymbol{I}_{14}=6\boldsymbol{X}-3\boldsymbol{X}^T\\ \boldsymbol{I}_{22}&=-n_2\boldsymbol{P}-n_3\boldsymbol{P}+\boldsymbol{X}+\boldsymbol{X}^T+h_1n_2\left(\boldsymbol{Y}_j\bar{\boldsymbol{C}}_i+\bar{\boldsymbol{C}}_i^T\boldsymbol{Y}_j^T\right)\\ \boldsymbol{I}_{23}&=2\boldsymbol{X}+\boldsymbol{X}^T,\quad \boldsymbol{I}_{24}=6\boldsymbol{X}+\boldsymbol{X}^T,\quad \boldsymbol{I}_{33}=2\boldsymbol{X}+2\boldsymbol{X}^T\\ \boldsymbol{I}_{34}&=6\boldsymbol{X}+2\boldsymbol{X}^T,\quad \boldsymbol{I}_{44}=6\boldsymbol{X}+6\boldsymbol{X}^T\\ \boldsymbol{I}'_{11}&=\boldsymbol{P}\bar{\boldsymbol{A}}_i+\bar{\boldsymbol{A}}_i^T\boldsymbol{P}-n_2\boldsymbol{P}+n_3\boldsymbol{P}-3\boldsymbol{X}-3\boldsymbol{X}^T\\ \boldsymbol{I}'_{12}&=-\boldsymbol{Y}_j\bar{\boldsymbol{C}}_i+n_2\boldsymbol{P}+\boldsymbol{X}-3\boldsymbol{X}^T\\ \boldsymbol{I}'_{22}&=-n_2\boldsymbol{P}-n_3\boldsymbol{P}+\boldsymbol{X}+\boldsymbol{X}^T\\ \boldsymbol{\Pi}_{11}&=\boldsymbol{P}\bar{\boldsymbol{A}}_i+\bar{\boldsymbol{A}}_i^T\boldsymbol{P}+n_3\boldsymbol{P}-n_2\boldsymbol{P}-3\boldsymbol{X}-3\boldsymbol{X}^T+h_1n_1\bar{\boldsymbol{A}}_i^T\boldsymbol{P}\bar{\boldsymbol{A}}_i\\ &\quad+h_1n_2\left(\boldsymbol{P}\bar{\boldsymbol{A}}_i+\bar{\boldsymbol{A}}_i^T\boldsymbol{P}\right)+\boldsymbol{I}\\ \boldsymbol{\Pi}_{12}&=\boldsymbol{I}_{12},\quad \boldsymbol{\Pi}_{13}=\boldsymbol{I}_{13},\quad \boldsymbol{\Pi}_{14}=\boldsymbol{I}_{14}\\ \boldsymbol{\Pi}_{15}&=\boldsymbol{Y}_j\boldsymbol{E}_{vi}+h_1n_1\bar{\boldsymbol{A}}_i^T\boldsymbol{Y}_j\boldsymbol{E}_{vi}+h_1n_2\boldsymbol{Y}_j\boldsymbol{E}_{vi}\\ \boldsymbol{\Pi}_{16}&=-\boldsymbol{P}\bar{\boldsymbol{E}}_{wi}-h_1n_1\bar{\boldsymbol{A}}_i^T\boldsymbol{P}\bar{\boldsymbol{E}}_{wi}-h_1n_2\boldsymbol{P}\bar{\boldsymbol{E}}_{wi}\\ \boldsymbol{\Pi}_{22}&=\boldsymbol{I}_{22},\quad \boldsymbol{\Pi}_{23}=\boldsymbol{I}_{23},\quad \boldsymbol{\Pi}_{24}=\boldsymbol{I}_{24},\quad \boldsymbol{\Pi}_{25}=-h_1n_2\boldsymbol{Y}_j\boldsymbol{E}_{vi}\end{aligned}$$

$$\Pi_{26} = h_1 n_1 \bar{C}^T Y^T \bar{E}_{wi} + h_1 n_2 P \bar{E}_{wi}, \quad \Pi_{27} = h_1 n_1 \bar{C}_i^T Y_j^T$$
$$\Pi_{33} = I_{33}, \quad \Pi_{34} = I_{34}, \ \Pi_{44} = I_{44}, \ \Pi_{55} = -\gamma_1^2 I$$
$$\Pi_{56} = -h_1 n_1 E_{vi}^T Y_j^T \bar{E}_{wi}, \quad \Pi_{57} = h_1 n_1 E_{vi}^T Y_j^T$$
$$\Pi_{66} = -\gamma_1^2 I + h_1 n_1 \bar{E}_{wi}^T P \bar{E}_{wi}, \quad \Pi_{77} = -h_1 n_1 P$$
$$\Pi'_{11} = I'_{11} + I, \ \Pi'_{12} = I'_{12}, \ \Pi'_{13} = I_{13}, \ \Pi'_{14} = I_{14}$$
$$\Pi'_{15} = Y_j E_{vi}, \ \Pi'_{16} = -P\bar{E}_{wi}, \ \Pi'_{23} = I_{23}, \ \Pi'_{24} = I_{24}$$
$$\Pi'_{22} = -n_3 P - n_2 P + X + X^T, \ \Pi'_{33} = I_{33}$$
$$\Pi'_{34} = I_{34}, \Pi'_{44} = I_{44}, \ \Pi'_{55} = -\gamma_1^2 I, \Pi'_{66} = -\gamma_1^2 I$$
$$\Pi'_{77} = -\frac{15 n_1}{23 h_1} P$$

Proof: In order to make the error system in Eq. (10) asymptotically stable, let $\bar{w}(t) = 0$ and $v(i_{k_1}) = 0$, and we construct the following Lyapunov functional:

$$\begin{aligned} V_1(t) = \bar{e}^T(t) P \bar{e}(t) + \int_{t-\tau_1(t)}^{t} \bar{e}^T(s) Q \bar{e}(s) ds \\ + (h_1 - \tau_1(t)) \int_{t-\tau_1(t)}^{t} \dot{\bar{e}}^T(s) R \dot{\bar{e}}(s) ds \\ + (h_1 - \tau_1(t)) \varphi_1^T(t) S \varphi_1(t) \end{aligned} \tag{15}$$

where, $\varphi_1(t) = \bar{e}(t) - \bar{e}(i_{k_1})$, $P = P^T > 0$, $Q = Q^T > 0$, $R = R^T > 0$, $S = S^T > 0$.

Taking the derivative of $V_1(t)$ along the trajectory of the system in Eq. (10):

$$\begin{aligned} \dot{V}_1(t) = 2\bar{e}^T(t) P \dot{\bar{e}}(t) + \bar{e}^T(t) Q \bar{e}(t) - \bar{e}^T(t - \tau_1(t)) Q \\ \times \bar{e}(t - \tau_1(t)) - \int_{t-\tau_1(t)}^{t} \dot{\bar{e}}^T(s) R \dot{\bar{e}}(s) ds - \varphi_1^T(t) S \varphi_1(t) \\ + (h_1 - \tau_1(t)) \dot{\bar{e}}^T(t) R \dot{\bar{e}}(t) + 2(h_1 - \tau_1(t)) \varphi_1^T(t) S \dot{\bar{e}}(t) \end{aligned} \tag{16}$$

The integral term $-\int_{t-\tau_1(t)}^{t} \dot{\bar{e}}^T(t) R \dot{\bar{e}}(s) ds$ in $\dot{V}_1(t)$ can be treated by introducing the affine Bessel-Legendre inequality in [35], [36], which is:

$$-\int_{t-\tau_1(t)}^{t} \dot{\bar{e}}^T(s) R \dot{\bar{e}}(s) ds \le -\psi_1^T(t) \Theta \psi_1(t) \tag{17}$$

where

$$\psi_1^T(t) = \begin{bmatrix} \bar{e}^T(t) & \bar{e}^T(i_{k_1}) & \frac{1}{\tau_1(t)} \Omega_0^T & \frac{1}{\tau_1(t)} \Omega_1^T \end{bmatrix},$$
$$\Theta = X H_2 + H_2^T X^T - \tau_1(t) X \bar{R} X^T, \quad \Omega_0 = \int_{t-\tau_1(t)}^{t} \bar{e}(s) ds,$$
$$\Omega_1 = \int_{t-\tau_1(t)}^{t} \left(2\frac{s - t + \tau_1(t)}{\tau_1(t)} - 1 \right) \bar{e}(s) ds,$$
$$\bar{R} = \operatorname{diag}\left\{ R^{-1} \quad \frac{1}{3} R^{-1} \quad \frac{1}{5} R^{-1} \right\} \quad \text{and}$$
$$H_2 = \begin{bmatrix} I & -I & 0 & 0 \\ I & I & -2I & 0 \\ I & -I & 0 & -6I \end{bmatrix}.$$

Substitute the inequality in Eq. (17) into $\dot{V}_1(t)$ and define:

$$M_{11} = \begin{bmatrix} I & 0 & 0 & 0 \end{bmatrix}, \quad M_{12} = \begin{bmatrix} I & -I & 0 & 0 \end{bmatrix},$$
$$M_{13} = \begin{bmatrix} \bar{A}_i & -\bar{L}_j \bar{C}_i & 0 & 0 \end{bmatrix} \quad \text{and} \quad M_{14} = \begin{bmatrix} 0 & I & 0 & 0 \end{bmatrix}.$$

Then, $\bar{e}(t) = M_{11}\psi_1(t)$, $\varphi_1(t) = M_{12}\psi_1(t)$, $\dot{\bar{e}}(t) = M_{13}\psi_1(t)$ and $\bar{e}(t - \tau_1(t)) = M_{14}\psi_1(t)$.

Therefore, the following can be obtained:

$$\dot{V}_1(t) \le \psi_1^T(t) \left[\Sigma_{11} + (h_1 - \tau_1(t)) \Sigma_{12} + \tau_1(t) \Sigma_{13} \right] \psi_1(t)$$

where

$$\begin{aligned} \Sigma_{11} &= 2M_{11}^T P M_{13} + M_{11}^T Q M_{11} - M_{14}^T Q M_{14} - M_{12}^T S M_{12} \\ &\quad - X H_2 - H_2^T X^T \end{aligned}$$
$$\Sigma_{12} = 2M_{12}^T S M_{13} + M_{13}^T R M_{13}, \ \Sigma_{13} = X \bar{R} X^T$$

If $\Sigma_{11} + (h_1 - \tau_1(t)) \Sigma_{12} + \tau_1(t) \Sigma_{13} < 0$, then $\dot{V}_1(t) < 0$, so the error system in Eq. (10) is asymptotically stable. According to the linear convex combination lemma, the necessary and sufficient conditions for the inequality $\Sigma_{11} + (h_1 - \tau_1(t)) \Sigma_{12} + \tau_1(t) \Sigma_{13} < 0$ to be true are:

$$\Sigma_{11} + h_1 \Sigma_{12} < 0, \ \Sigma_{11} + h_1 \Sigma_{13} < 0 \tag{18}$$

Under the zero initial condition, when $\bar{w}(t) \neq 0$, $v(i_{k_1}) \neq 0$, considering the following performance index function:

$$J_1 = \dot{V}_1(t) + \bar{e}^T(t) \bar{e}(t) - \gamma_1^2 (v^T(i_{k_1}) v(i_{k_1}) + \bar{w}^T(t) \bar{w}(t)) < 0 \tag{19}$$

Define

$$\psi_2^T(t) = \begin{bmatrix} \bar{e}^T(t) & \bar{e}^T(t - \tau_1(t)) & \frac{1}{\tau_1(t)} \Omega_0^T \\ \frac{1}{\tau_1(t)} \Omega_1^T & v^T(t - \tau_1(t)) & \bar{w}^T(t) \end{bmatrix}$$
$$M_{21} = \begin{bmatrix} I & 0 & 0 & 0 & 0 & 0 \end{bmatrix}$$
$$M_{22} = \begin{bmatrix} I & -I & 0 & 0 & 0 & 0 \end{bmatrix}$$
$$M_{23} = \begin{bmatrix} \bar{A}_i & -\bar{L}_j \bar{C}_i & 0 & 0 & \bar{L}_j E_{vi} & -\bar{E}_{wi} \end{bmatrix}$$
$$M_{24} = \begin{bmatrix} 0 & I & 0 & 0 & 0 & 0 \end{bmatrix}$$
$$M_{25} = \begin{bmatrix} I & 0 & 0 & 0 & 0 & 0 \\ 0 & I & 0 & 0 & 0 & 0 \\ 0 & 0 & I & 0 & 0 & 0 \\ 0 & 0 & 0 & I & 0 & 0 \end{bmatrix}$$
$$M_{26} = \begin{bmatrix} 0 & 0 & 0 & 0 & I & 0 \\ 0 & 0 & 0 & 0 & 0 & I \end{bmatrix}$$

Ω_0, Ω_1 are similar to in Eq. (17), then:

$$\bar{e}(t) = M_{21}\psi_2(t), \quad \varphi_1(t) = M_{22}\psi_2(t), \dot{\bar{e}}(t) = M_{23}\psi_2(t),$$
$$\bar{e}(t - \tau_1(t)) = M_{24}\psi_2(t), \quad \psi_1(t) = M_{25}\psi_2(t),$$
$$\begin{bmatrix} v^T(i_k) & \bar{w}^T(t) \end{bmatrix}^T = M_{26}\psi_2(t).$$

It is derived that:

$$J_1 = \psi_2^T(t) \left[\Sigma_{21} + (h_1 - \tau_1(t)) \Sigma_{22} + \tau_1(t) \Sigma_{23} \right] \psi_2(t) < 0 \tag{20}$$

where,

$$\begin{aligned} \Sigma_{21} = 2M_{23}^T P M_{21} + M_{21}^T Q M_{21} - M_{24}^T Q M_{24} + M_{21}^T M_{21} \\ - M_{25}^T \left(X H_2 + H_2^T X^T \right) M_{25} - M_{22}^T S M_{22} - \gamma_1^2 M_{26}^T M_{26} \end{aligned}$$

$$\boldsymbol{\Sigma}_{22}=\boldsymbol{M}_{23}^T\boldsymbol{R}\boldsymbol{M}_{23}+2\boldsymbol{M}_{22}^T\boldsymbol{S}\boldsymbol{M}_{23},\quad \boldsymbol{\Sigma}_{23}=\boldsymbol{M}_{25}^T\boldsymbol{X}\bar{\boldsymbol{R}}\boldsymbol{X}^T\boldsymbol{M}_{25}$$

It can be seen from the linear convex combination lemma that $J_1<0$ is equivalent to:

$$\boldsymbol{\Sigma}_{21}+h_1\boldsymbol{\Sigma}_{22}<\boldsymbol{0},\quad \boldsymbol{\Sigma}_{21}+h_1\boldsymbol{\Sigma}_{23}<\boldsymbol{0} \tag{21}$$

Since the inequalities (18) and (20) are nonlinear, let $\boldsymbol{R}=n_1\boldsymbol{P},\boldsymbol{S}=n_2\boldsymbol{P},\boldsymbol{Q}=n_3\boldsymbol{P},\boldsymbol{Y}_j=\boldsymbol{P}\bar{\boldsymbol{L}}_j$, then the nonlinear inequalities can be transformed into linear matrix inequalities by applying the Schur complementary lemma. In addition, we can use LMI toolbox to obtain feasible solution in Eq. (11)–(14). The parameters $\boldsymbol{L}_j$ and $\boldsymbol{F}_j$ to be obtained by solving $\bar{\boldsymbol{L}}_j=\boldsymbol{P}^{-1}\boldsymbol{Y}_j$.

The Eq. (19) is integrated from 0 to $+\infty$, then the following inequality can be obtained.

$$\begin{aligned}V_1(+\infty)-V_1(0)\le&-\int_0^{+\infty}\bar{e}^T(s)\bar{e}(s)ds+\gamma_1^2\int_0^{+\infty}\bar{w}^T(s)\bar{w}(s)ds\\&+\gamma_1^2\sum_{k=0}^{+\infty}\left[\left(i_{k_1+1}-i_k\right)v^T(i_{k_1})v(i_{k_1})\right]\end{aligned}$$

where $\bar{w}(t)\in\boldsymbol{L}_2[0,+\infty)$, $v(i_{k_1})\in\boldsymbol{L}_2[0,+\infty)$, $V_1(0)=0$, $V_1(+\infty)\ge 0$.

Therefore, $\|\bar{e}(t)\|_2^2\le\gamma_1^2[\sum_{k=0}^{+\infty}(i_{k_1+1}-i_{k_1})\|v(i_{k_1})\|_2^2+\|\bar{w}(t)\|_2^2]$ is true. So far, H_∞ relevant performance indicators have been proved.

IV. CO-DESIGN OF DUAL SECURITY CONTROL AND COMMUNICATION FOR CPS

Considering that the CPS suffered from DoS attack, and after the state and fault estimation through Theorem 1 are obtained, the following dynamic output feedback controller with fault adjustment ability is constructed:

$$\begin{aligned}u(t)=\sum_{i=1}^r\sum_{j=1}^r\xi_i(\theta(t))\xi_j(\theta(t))[&\boldsymbol{K}_j\hat{x}(t-\tau_2(t))\\&-\boldsymbol{B}_j^+\boldsymbol{E}_{fi}\hat{f}(t-\tau_2(t))]\end{aligned} \tag{22}$$

where $t\in\left[j_{k_3},j_{k_3+1}\right)$, the gain matrix of the dynamic output feedback controller is $\boldsymbol{K}_j\in\boldsymbol{R}^{n_u\times n}$ and the fault adjustment matrix $\boldsymbol{B}_j^+\in\boldsymbol{R}^{n_u\times n}$ satisfy $\left(\boldsymbol{I}-\boldsymbol{B}_i\boldsymbol{B}_j^+\right)\boldsymbol{E}_{fi}=0$, that is, $rank\left(\boldsymbol{B}_i,\boldsymbol{E}_{fi}\right)=rank(\boldsymbol{B}_i)$. By substituting Eq. (22) into Eq. (2), a closed-loop nonlinear CPS model that integrates actuator fault, DoS attack, fault tolerance and attack tolerance under DETCS can be obtained as follows:

$$\begin{aligned}\dot{x}(t)=\sum_{i=1}^r\sum_{j=1}^r&\xi_i(\theta(t))\xi_j(\theta(t))[\boldsymbol{A}_ix(t)+\boldsymbol{B}_i\boldsymbol{K}_jx(t-\tau_2(t))\\&+\boldsymbol{B}_i\boldsymbol{K}_je_x\left(t-\tau_2(t)\right)-\boldsymbol{E}_{fi}e_f\left(t-\tau_2(t)\right)+\boldsymbol{E}_{\boldsymbol{wi}}w\left(t\right)\\&+\tau_2(t)\boldsymbol{E}_{fi}\dot{f}\left(t\right)]\end{aligned} \tag{23}$$

Theorem 2: Based on DETCS, given positive numbers h_2 and γ_2, for the system in Eq.(23) with continuous time-varying actuator fault $f\left(t\right)$ and DoS attack, if there exist symmetric positive definite matrix $\tilde{\boldsymbol{P}}>\boldsymbol{0}$ and appropriate dimension matrices $\tilde{\boldsymbol{X}},\boldsymbol{K}_{1j},\boldsymbol{Q}_1,\boldsymbol{Q}_3,\boldsymbol{Q}_5$, then the following inequalities hold:

$$\begin{bmatrix}\Xi_{11}&\Xi_{12}&\Xi_{13}&\Xi_{14}&\boldsymbol{0}&\boldsymbol{0}\\ *&\Xi_{22}&\Xi_{23}&\Xi_{24}&\Xi_{25}&\Xi_{26}\\ *&*&\Xi_{33}&\Xi_{34}&\boldsymbol{0}&\boldsymbol{0}\\ *&*&*&\Xi_{44}&\boldsymbol{0}&\boldsymbol{0}\\ *&*&*&*&\Xi_{55}&\boldsymbol{0}\\ *&*&*&*&*&\Xi_{66}\end{bmatrix}<\boldsymbol{0} \tag{24}$$

$$\begin{bmatrix}\Xi'_{11}&\Xi'_{12}&\Xi_{13}&\Xi_{14}&\boldsymbol{0}&\tilde{\boldsymbol{X}}\\ *&\Xi'_{22}&\Xi_{23}&\Xi_{24}&\Xi_{25}&\tilde{\boldsymbol{X}}\\ *&*&\Xi_{33}&\Xi_{34}&\boldsymbol{0}&\tilde{\boldsymbol{X}}\\ *&*&*&\Xi_{44}&\boldsymbol{0}&\tilde{\boldsymbol{X}}\\ *&*&*&*&\Xi_{55}&\boldsymbol{0}\\ *&*&*&*&*&\Xi'_{66}\end{bmatrix}<\boldsymbol{0} \tag{25}$$

$$\begin{bmatrix}\boldsymbol{Z}_{11}&\boldsymbol{Z}_{12}\\ *&\boldsymbol{Z}_{22}\end{bmatrix}<\boldsymbol{0} \tag{26}$$

$$\begin{bmatrix}\boldsymbol{Z}'_{11}&\boldsymbol{Z}'_{12}\\ *&\boldsymbol{Z}'_{22}\end{bmatrix}<\boldsymbol{0} \tag{27}$$

$$\begin{bmatrix}\boldsymbol{Q}_1&\boldsymbol{E}_{fi}^T\tilde{\boldsymbol{P}}\\ *&m_1\tilde{\boldsymbol{P}}\end{bmatrix}>\boldsymbol{0},\quad\begin{bmatrix}\boldsymbol{Q}_3&n_{11}\boldsymbol{E}_{fi}^T\tilde{\boldsymbol{P}}\\ *&m_2\tilde{\boldsymbol{P}}\end{bmatrix}>\boldsymbol{0},$$

$$\begin{bmatrix}\boldsymbol{Q}_5&n_2\boldsymbol{E}_{fi}^T\tilde{\boldsymbol{P}}\\ *&m_3\tilde{\boldsymbol{P}}\end{bmatrix}>\boldsymbol{0} \tag{28}$$

Then the system in Eq. (23) is asymptotically stable and meets the following performance indexes:

$$\begin{aligned}\parallel x(t)\parallel_2^2\le\gamma_2^2[&\parallel\bar{w}(t)\parallel_2^2\\&+\sum_{k=0}^{+\infty}\left(j_{k_3+1}-j_{k_3}\right)\left(\parallel e_x(j_{k_3})\parallel_2^2+\parallel e_f(j_{k_3})\parallel_2^2\right)]\end{aligned}$$

The controller gain $\boldsymbol{K}_j=(\tilde{\boldsymbol{P}}\boldsymbol{B}_i)^{-1}\boldsymbol{K}_{1j}$ with attack tolerance and event trigger weight matrix $\boldsymbol{\Phi}$ can be obtained cooperatively, and the fault compensation matrix satisfies $\left(\boldsymbol{I}-\boldsymbol{B}_i\boldsymbol{B}_j^+\right)\boldsymbol{E}_{fi}=\boldsymbol{0}$.

where

$$\begin{aligned}\Xi_{11}=&\tilde{\boldsymbol{P}}\boldsymbol{A}_i+\boldsymbol{A}_i^T\tilde{\boldsymbol{P}}+n_3\tilde{\boldsymbol{P}}-n_1\tilde{\boldsymbol{P}}+\frac{h_2^2}{4}m_3\boldsymbol{A}_i^T\tilde{\boldsymbol{P}}\boldsymbol{A}_i+\frac{h_2^2}{4}m_2\tilde{\boldsymbol{P}}\\&+h_2n_2\boldsymbol{A}_i^T\tilde{\boldsymbol{P}}\boldsymbol{A}_i+h_2n_1\left(\tilde{\boldsymbol{P}}\boldsymbol{A}_i+\boldsymbol{A}_i^T\tilde{\boldsymbol{P}}\right)-3\tilde{\boldsymbol{X}}-3\tilde{\boldsymbol{X}}^T\end{aligned}$$

$$\begin{aligned}\Xi_{12}=&\boldsymbol{K}_{1j}+n_1\tilde{\boldsymbol{P}}+\frac{h_2^2}{4}m_3\boldsymbol{A}_i^T\boldsymbol{K}_{1j}-\frac{h_2^2}{4}m_2\tilde{\boldsymbol{P}}+h_2n_2\boldsymbol{A}_i^T\boldsymbol{K}_{1j}\\&+h_2n_1\boldsymbol{K}_{1j}-h_2n_1\boldsymbol{A}_i^T\tilde{\boldsymbol{P}}+\tilde{\boldsymbol{X}}-3\tilde{\boldsymbol{X}}^T\end{aligned}$$

$$\Xi_{13}=2\tilde{\boldsymbol{X}}-3\tilde{\boldsymbol{X}}^T,\quad\Xi_{14}=6\tilde{\boldsymbol{X}}-3\tilde{\boldsymbol{X}}^T$$

$$\Xi_{22}=-n_3\tilde{\boldsymbol{P}}-n_1\tilde{\boldsymbol{P}}+\frac{h_2^2}{4}m_2\tilde{\boldsymbol{P}}-h_2n_1\left(\boldsymbol{K}_{1j}+\boldsymbol{K}_{1j}^T\right)+\tilde{\boldsymbol{X}}+\tilde{\boldsymbol{X}}^T$$

$$\Xi_{23}=2\tilde{\boldsymbol{X}}+\tilde{\boldsymbol{X}}^T,\quad\Xi_{24}=6\tilde{\boldsymbol{X}}+\tilde{\boldsymbol{X}}^T,\quad\Xi_{25}=\frac{h_2^2}{4}m_3\boldsymbol{K}_{1j}^T$$

$$\Xi_{26}=h_2n_2\boldsymbol{K}_{1j}^T,\quad\Xi_{33}=2\tilde{\boldsymbol{X}}+2\tilde{\boldsymbol{X}}^T,\quad\Xi_{34}=6\tilde{\boldsymbol{X}}+2\tilde{\boldsymbol{X}}^T,$$

$$\Xi_{44}=6\tilde{\boldsymbol{X}}+6\tilde{\boldsymbol{X}}^T,\quad\Xi_{55}=-\frac{h_2^2}{4}m_3\tilde{\boldsymbol{P}},\quad\Xi_{66}=-h_2n_2\tilde{\boldsymbol{P}}$$

$$\Xi'_{11} = \tilde{P}A_i + A_i^T\tilde{P} + n_3\tilde{P} - n_1\tilde{P} + \frac{h_2^2}{4}m_3A_i^T\tilde{P}A_i + \frac{h_2^2}{4}m_2\tilde{P} + h_2m_1\tilde{P} - 3\tilde{X} - 3\tilde{X}^T$$

$$\Xi'_{12} = K_{1j} + n_1\tilde{P} + \frac{h_2^2}{4}m_3A_i^TK_{1j} - \frac{h_2^2}{4}m_2\tilde{P} + \tilde{X} - 3\tilde{X}^T$$

$$\Xi'_{22} = -n_3\tilde{P} - n_1\tilde{P} + \frac{h_2^2}{4}m_2\tilde{P} + \tilde{X} + \tilde{X}^T, \quad \Xi'_{66} = -\frac{15n_2}{23h_2}\tilde{P}$$

$$\Psi_{11} = \Xi_{11} + I, \quad \Psi_{12} = \Xi_{12}, \quad \Psi_{13} = \Xi_{13}, \quad \Psi_{14} = \Xi_{14}$$

$$\Psi_{15} = K_{1j} + \frac{h_2^2}{4}m_3A_i^TK_{1j} + h_2n_2A_i^TK_{1j} + h_2n_1K_{1j}$$

$$Z_{11} = \begin{bmatrix} \Psi_{11} & \Psi_{12} & \Psi_{13} & \Psi_{14} & \Psi_{15} & \Psi_{16} \\ * & \Psi_{22} & \Psi_{23} & \Psi_{24} & \Psi_{25} & \Psi_{26} \\ * & * & \Psi_{33} & \Psi_{34} & 0 & 0 \\ * & * & * & \Psi_{44} & 0 & 0 \\ * & * & * & * & \Psi_{55} & \Psi_{56} \\ * & * & * & * & * & \Psi_{66} \end{bmatrix}$$

$$Z_{12} = \begin{bmatrix} \Psi_{17} & 0 & 0 & 0 & 0 \\ \Psi_{27} & 0 & 0 & \frac{h_2^2}{4}m_3K_{1j}^T & h_2n_2K_{1j}^T \\ 0 & 0 & 0 & 0 & 0 \\ 0 & 0 & 0 & 0 & 0 \\ \Psi_{57} & 0 & 0 & \frac{h_2^2}{4}m_3K_{1j}^T & h_2n_2K_{1j}^T \\ \Psi_{67} & 0 & 0 & 0 & 0 \end{bmatrix}$$

$$Z_{22} = \begin{bmatrix} \Psi_{77} & 0 & 0 & 0 & 0 \\ * & \delta_s\Phi & 0 & 0 & 0 \\ * & * & -\Phi & 0 & 0 \\ * & * & * & -\frac{h_2^2}{4}m_3\tilde{P} & 0 \\ * & * & * & * & -h_2n_2\tilde{P} \end{bmatrix}$$

$$\Psi_{16} = -\tilde{P}E_{fi} - \frac{h_2^2}{4}m_3A_i^T\tilde{P}E_{fi} - h_2n_2A_i^T\tilde{P}E_{fi} - h_2n_1\tilde{P}E_{fi}$$

$$\Psi_{17} = \tilde{P}E_{wi} + \frac{h_2^2}{4}m_3A_i^T\tilde{P}E_{wi} + h_2n_2A_i^T\tilde{P}E_{wi} + h_2n_1\tilde{P}E_{wi}$$

$$\Psi_{22} = -n_3\tilde{P} - n_1\tilde{P} + \tilde{X} + \tilde{X}^T + \frac{h_2^2}{4}m_2\tilde{P} - h_2n_1(K_{1j} + K_{1j}^T)$$

$$\Psi_{23} = \Xi_{23}, \quad \Psi_{24} = \Xi_{24}, \quad \Psi_{25} = -h_2n_1K_{1j}$$

$$\Psi_{26} = -\frac{h_2^2}{4}m_3K_{1j}^TE_{fi} - h_2n_2K_{1j}^TE_{fi} + h_2n_1\tilde{P}E_{fi}$$

$$\Psi_{27} = \frac{h_2^2}{4}m_3K_{1j}^TE_{wi} + h_2n_2K_{1j}^TE_{wi} - h_2n_1\tilde{P}E_{wi}$$

$$\Psi_{33} = \Xi_{33}, \quad \Psi_{34} = \Xi_{34}, \quad \Psi_{44} = \Xi_{44}, \quad \Psi_{55} = -\gamma_2^2I$$

$$\Psi_{56} = -\frac{h_2^2}{4}m_3K_{1j}^TE_{fi} - h_2n_2K_{1j}^TE_{fi}$$

$$\Psi_{57} = \frac{h_2^2}{4}m_3K_{1j}^TE_{wi} + h_2n_2K_{1j}^TE_{wi}$$

$$\Psi_{66} = -\gamma_2^2I + \frac{h_2^2}{4}m_3E_{fi}^T\tilde{P}E_{fi} + h_2n_2E_{fi}^T\tilde{P}E_{fi}$$

$$\Psi_{67} = -\frac{h_2^2}{4}m_3E_{fi}^T\tilde{P}E_{wi} - h_2n_2E_{fi}^T\tilde{P}E_{wi}$$

$$\Psi_{77} = -\gamma_2^2I + \frac{h_2^2}{4}m_3E_{wi}^T\tilde{P}E_{wi} + h_2n_2E_{wi}^T\tilde{P}E_{wi}$$

$$\Psi'_{11} = \Xi'_{11} + I, \quad \Psi'_{12} = \Xi'_{12}, \; \Psi'_{13} = \Xi'_{13}, \; \Psi'_{14} = \Xi'_{14}$$

$$\Psi'_{15} = K_{1j} + \frac{h_2^2}{4}m_3A_i^TK_{1j}$$

$$Z'_{11} = \begin{bmatrix} \Psi'_{11} & \Psi'_{12} & \Psi'_{13} & \Psi'_{14} & \Psi'_{15} & \Psi'_{16} \\ * & \Psi'_{22} & \Psi'_{23} & \Psi'_{24} & 0 & \Psi'_{26} \\ * & * & \Psi'_{33} & \Psi'_{34} & 0 & 0 \\ * & * & * & \Psi'_{44} & 0 & 0 \\ * & * & * & * & \Psi'_{55} & \Psi'_{56} \\ * & * & * & * & * & \Psi'_{66} \end{bmatrix}$$

$$Z'_{12} = \begin{bmatrix} \Psi'_{17} & 0 & 0 & \tilde{X} & 0 \\ \Psi'_{27} & 0 & 0 & \tilde{X} & \frac{h_2^2}{4}m_3K_{1j}^T \\ 0 & 0 & 0 & \tilde{X} & 0 \\ 0 & 0 & 0 & \tilde{X} & 0 \\ \Psi'_{57} & 0 & 0 & 0 & \frac{h_2^2}{4}m_3K_{1j}^T \\ \Psi'_{67} & 0 & 0 & 0 & 0 \end{bmatrix}$$

$$Z'_{22} = \begin{bmatrix} \Psi'_{77} & 0 & 0 & 0 & 0 \\ * & \delta_s\Phi & 0 & 0 & 0 \\ * & * & -\Phi & 0 & 0 \\ * & * & * & -\frac{15n_2}{23h_2}\tilde{P} & 0 \\ * & * & * & * & -\frac{h_2^2}{4}m_3\tilde{P} \end{bmatrix}$$

$$\Psi'_{16} = -\tilde{P}E_{fi} - \frac{h_2^2}{4}m_3A_i^T\tilde{P}E_{fi}$$

$$\Psi'_{17} = \tilde{P}E_{wi} + \frac{h_2^2}{4}m_3A_i^T\tilde{P}E_{wi}$$

$$\Psi'_{22} = -n_3\tilde{P} - n_1\tilde{P} + \tilde{X} + \tilde{X}^T + \frac{h_2^2}{4}m_2\tilde{P}$$

$$\Psi'_{23} = \Xi_{23}, \quad \Psi'_{24} = \Xi_{24}, \quad \Psi_{26} = -\frac{h_2^2}{4}m_3K_{1j}^TE_{fi}$$

$$\Psi'_{27} = -\frac{h_2^2}{4}m_3K_{1j}^TE_{wi}, \quad \Psi'_{33} = \Xi_{33}, \quad \Psi'_{34} = \Xi_{34}, \quad \Psi'_{44} = \Xi_{44}$$

$$\Psi_{55} = \Psi'_{55}, \quad \Psi'_{56} = -\frac{h_2^2}{4}m_3K_{1j}^TE_{fi}, \quad \Psi'_{57} = \frac{h_2^2}{4}m_3K_{1j}^TE_{wi}$$

$$\Psi_{66} = -\gamma_2^2I + \frac{h_2^2}{4}m_3E_{fi}^T\tilde{P}E_{fi} \quad \text{and} \quad \Psi'_{67} = -\frac{h_2^2}{4}m_3E_{fi}^T\tilde{P}E_{wi}$$

$$\Psi'_{77} = -\gamma_2^2I + \frac{h_2^2}{4}m_3E_{wi}^T\tilde{P}E_{wi}$$

Proof: Considering $e_x(j_{k_3}) = 0$, $e_f(j_{k_3}) = 0$ and $w(t) = 0$, we construct the following Lyapunov functional:

$$V_2(t) = x^T(t)\tilde{P}x(t) + (h_2 - \tau_2(t))\int_{t-\tau_2(t)}^{t}\dot{x}^T(s)\tilde{R}\dot{x}(s)ds + \int_{t-\tau_2(t)}^{t}x^T(s)\tilde{Q}x(s)ds + (h_2 - \tau_2(t))\varphi_2^T(t)\tilde{S}\varphi_2(t) \tag{29}$$

where $\tilde{P} = \tilde{P}^T > 0$, $\tilde{Q} = \tilde{Q}^T > 0$, $\tilde{R} = \tilde{R}^T > 0$, $\tilde{S} = \tilde{S}^T > 0$ and $\varphi_2(t) = x(t) - x(j_{k_3})$.

Taking the derivative $V_2(t)$ along the trajectory of the system in Eq. (29):

$$\begin{aligned}\dot{V}_2(t)=&2x^T(t)\tilde{\boldsymbol{P}}\dot{x}(t)+x^T(t)\tilde{\boldsymbol{Q}}x(t)-x^T(t-\tau_2(t))\tilde{\boldsymbol{Q}}x(t-\tau_2(t))\\&-\int_{t-\tau_2(t)}^{t}\dot{x}^T(s)\tilde{\boldsymbol{R}}\dot{x}(s)ds+(h_2-\tau_2(t))\dot{x}^T(t)\tilde{\boldsymbol{R}}\dot{x}(t)\\&-\varphi_2^T(t)\tilde{\boldsymbol{S}}\varphi_2(t)+2(h_2-\tau_2(t))\varphi_2^T(t)\tilde{\boldsymbol{S}}\dot{x}(t)\end{aligned}\tag{30}$$

We adopt an affine Bessel-Legendre inequality to deal with the integral term in Eq. (30):

$$-\int_{t-\tau_2(t)}^{t}\dot{x}^T(s)\tilde{\boldsymbol{P}}\dot{x}(s)ds\leq-\psi_3^T(t)\tilde{\boldsymbol{\Theta}}\psi_3(t)\tag{31}$$

where

$$\begin{aligned}\psi_3^T(t)&=\begin{bmatrix}x^T(t) & x^T(t-\tau_2(t)) & \frac{1}{\tau_2(t)}\tilde{\boldsymbol{\Omega}}_0^T & \frac{1}{\tau_2(t)}\tilde{\boldsymbol{\Omega}}_1^T\end{bmatrix},\\ \tilde{\boldsymbol{\Omega}}_0&=\int_{t-\tau_2(t)}^{t}x(s)ds,\\ \tilde{\boldsymbol{\Omega}}_1&=\int_{t-\tau_2(t)}^{t}\left(2\frac{s-t+\tau_2(t)}{\tau_2(t)}-1\right)x(s)ds,\\ \tilde{\boldsymbol{\Theta}}&=\tilde{\boldsymbol{X}}\boldsymbol{H}_2+\boldsymbol{H}_2^T\tilde{\boldsymbol{X}}^T-\tau_2(t)\tilde{\boldsymbol{X}}\tilde{\tilde{\boldsymbol{R}}}\tilde{\boldsymbol{X}}^T,\\ \boldsymbol{H}_2&=\begin{bmatrix}\boldsymbol{I} & -\boldsymbol{I} & 0 & 0\\ \boldsymbol{I} & \boldsymbol{I} & -2\boldsymbol{I} & 0\\ \boldsymbol{I} & -\boldsymbol{I} & 0 & -6\boldsymbol{I}\end{bmatrix}.\end{aligned}$$

Define: $\boldsymbol{M}_{31}=\begin{bmatrix}\boldsymbol{I} & 0 & 0 & 0\end{bmatrix}$, $\boldsymbol{M}_{32}=\begin{bmatrix}\boldsymbol{I} & -\boldsymbol{I} & 0 & 0\end{bmatrix}$ $\boldsymbol{M}_{33}=\begin{bmatrix}\boldsymbol{A}_i & \boldsymbol{B}_i\boldsymbol{K}_j & 0 & 0\end{bmatrix}$, and $\boldsymbol{M}_{34}=\begin{bmatrix}0 & \boldsymbol{I} & 0 & 0\end{bmatrix}$ Then,

$$\begin{aligned}&x(t)=\boldsymbol{M}_{31}\psi_3(t),\quad \varphi_2(t)=\boldsymbol{M}_{32}\psi_3(t),\\&\dot{x}(t)=\boldsymbol{M}_{33}\psi_3(t)+\tau_2(t)\boldsymbol{E}_{fi}\dot{f}(t),\quad x(t-\tau_2(t))=\boldsymbol{M}_{34}\psi_3(t).\end{aligned}$$

So, we obtain

$$\begin{aligned}\dot{V}_2(t)\leq&\ \psi_3^T(t)\Big[2\boldsymbol{M}_{31}^T\tilde{\boldsymbol{P}}\boldsymbol{M}_{33}+\boldsymbol{M}_{31}^T\tilde{\boldsymbol{Q}}\boldsymbol{M}_{31}-\boldsymbol{M}_{32}^T\tilde{\boldsymbol{S}}\boldsymbol{M}_{32}\\&-\boldsymbol{M}_{34}^T\tilde{\boldsymbol{Q}}\boldsymbol{M}_{34}-(\tilde{\boldsymbol{X}}\boldsymbol{H}_2+\boldsymbol{H}_2^T\tilde{\boldsymbol{X}}^T)+(h_2-\tau_2(t))\\&\times(2\boldsymbol{M}_{32}^T\tilde{\boldsymbol{S}}\boldsymbol{M}_{33}+\boldsymbol{M}_{33}^T\tilde{\boldsymbol{R}}\boldsymbol{M}_{33})+\tau_2(t)\tilde{\boldsymbol{X}}\tilde{\tilde{\boldsymbol{R}}}\tilde{\boldsymbol{X}}^T\Big]\psi_3(t)\\&+2\tau_2(t)\psi_3^T(t)\boldsymbol{M}_{31}^T\tilde{\boldsymbol{P}}\boldsymbol{E}_{fi}\dot{f}(t)\\&+2(h_2-\tau_2(t))\tau_2(t)\psi_3^T(t)\boldsymbol{M}_{32}^T\tilde{\boldsymbol{S}}\boldsymbol{E}_{fi}\dot{f}(t)\\&+2(h_2-\tau_2(t))\tau_2(t)\psi_3^T(t)\boldsymbol{M}_{33}^T\tilde{\boldsymbol{R}}\boldsymbol{E}_{fi}\dot{f}(t)\\&+(h_2-\tau_2(t))\tau_2^2(t)\dot{f}^T(t)\boldsymbol{E}_{fi}^T\tilde{\boldsymbol{R}}\boldsymbol{E}_{fi}\dot{f}(t)\end{aligned}\tag{32}$$

According to the inequalities $\begin{bmatrix}\boldsymbol{Q_1} & \boldsymbol{E}_{fi}^T\tilde{\boldsymbol{P}}\\ * & \boldsymbol{Q_2}\end{bmatrix}>\boldsymbol{0}$, $\begin{bmatrix}\boldsymbol{Q_3} & \boldsymbol{E}_{fi}^T\tilde{\boldsymbol{S}}\\ * & \boldsymbol{Q_4}\end{bmatrix}>\boldsymbol{0}$, $\begin{bmatrix}\boldsymbol{Q_5} & \boldsymbol{E}_{fi}^T\tilde{\boldsymbol{R}}\\ * & \boldsymbol{Q_6}\end{bmatrix}>\boldsymbol{0}$ and the Moon inequality, we have

$$\begin{aligned}&2\tau_2(t)\psi_3^T(t)\boldsymbol{M}_{31}^T\tilde{\boldsymbol{P}}\boldsymbol{E}_{fi}\dot{f}(t)\\&\quad\leq\tau_2(t)x^T(t)\boldsymbol{Q}_2x(t)+\tau_2(t)\dot{f}^T(t)\boldsymbol{Q}_1\dot{f}(t)\\&\quad\leq\tau_2(t)x^T(t)\boldsymbol{Q}_2x(t)+h_2f_1^2\lambda_{\max}\left(\boldsymbol{Q}_1\right)\end{aligned}\tag{33}$$

$$\begin{aligned}&(h_2-\tau_2(t))\tau_2^2(t)\dot{f}^T(t)\boldsymbol{E}_{fi}^T\tilde{\boldsymbol{R}}\boldsymbol{E}_{fi}\dot{f}(t)\\&\quad\leq\frac{h_2^3}{8}f_1^2\lambda_{\max}\left(\boldsymbol{E}_{fi}^T\tilde{\boldsymbol{R}}\boldsymbol{E}_{fi}\right)\end{aligned}\tag{34}$$

$$\begin{aligned}&2(h_2-\tau_2(t))\tau_2(t)\psi_3^T(t)\boldsymbol{M}_{32}^T\tilde{\boldsymbol{S}}\boldsymbol{E}_{fi}\dot{f}(t)\\&\quad\leq\frac{h_2^2}{4}\left(\varphi_2^T(t)\boldsymbol{Q}_4\varphi_2(t)+\dot{f}^T(t)\boldsymbol{Q}_3\dot{f}(t)\right)\\&\quad\leq\frac{h_2^2}{4}\varphi_2^T(t)\boldsymbol{Q}_4\varphi_2(t)+\frac{h_2^2}{4}f_1^2\lambda_{\max}\left(\boldsymbol{Q}_3\right)\end{aligned}\tag{35}$$

$$\begin{aligned}&2(h_2-\tau_2(t))\tau_2(t)\psi_3^T(t)\boldsymbol{M}_{33}^T\tilde{\boldsymbol{R}}\boldsymbol{E}_{fi}\dot{f}(t)\\&\quad\leq\frac{h_2^2}{4}\left(\psi_3^T(t)\boldsymbol{M}_{33}^T\boldsymbol{Q}_6\boldsymbol{M}_{33}\psi_3(t)+\dot{f}^T(t)\boldsymbol{Q}_5\dot{f}(t)\right)\\&\quad\leq\frac{h_2^2}{4}\psi_3^T(t)\boldsymbol{M}_{33}^T\boldsymbol{Q}_6\boldsymbol{M}_{33}\psi_3(t)+\frac{h_2^2}{4}f_1^2\lambda_{\max}\left(\boldsymbol{Q}_5\right)\end{aligned}\tag{36}$$

By substituting inequalities (33)–(36) into (32), we get:

$$\begin{aligned}\dot{V}_2(t)\leq&\ \psi_3^T(t)\Big[2\boldsymbol{M}_{31}^T\tilde{\boldsymbol{P}}\boldsymbol{M}_{33}-\boldsymbol{M}_{32}^T\tilde{\boldsymbol{S}}\boldsymbol{M}_{32}+\boldsymbol{M}_{31}^T\tilde{\boldsymbol{Q}}\boldsymbol{M}_{31}\\&-\boldsymbol{M}_{34}^T\tilde{\boldsymbol{Q}}\boldsymbol{M}_{34}-(\tilde{\boldsymbol{X}}\boldsymbol{H}_2+\boldsymbol{H}_2^T\tilde{\boldsymbol{X}}^T)+\frac{h_2^2}{4}\boldsymbol{M}_{32}^T\boldsymbol{Q}_4\boldsymbol{M}_{32}\\&+\frac{h_2^2}{4}\boldsymbol{M}_{33}^T\boldsymbol{Q}_6\boldsymbol{M}_{33}+(h_2-\tau_2(t))(2\boldsymbol{M}_{32}^T\tilde{\boldsymbol{S}}\boldsymbol{M}_{33}\\&+\boldsymbol{M}_{33}^T\tilde{\boldsymbol{R}}\boldsymbol{M}_{33})+\tau_2(t)(\tilde{\boldsymbol{X}}\tilde{\tilde{\boldsymbol{R}}}\tilde{\boldsymbol{X}}^T+\boldsymbol{M}_{31}^T\boldsymbol{Q}_2\boldsymbol{M}_{31})\Big]\psi_3(t)+\nu\\=&\ \psi_3^T(t)\left[\boldsymbol{\Sigma}_{31}+(h_2-\tau_2(t))\boldsymbol{\Sigma}_{32}+\tau_2(t)\boldsymbol{\Sigma}_{33}\right]\psi_3(t)+\nu\end{aligned}\tag{37}$$

where

$$\begin{aligned}\boldsymbol{\Sigma}_{31}=&\ 2\boldsymbol{M}_{31}^T\tilde{\boldsymbol{P}}\boldsymbol{M}_{33}-\boldsymbol{M}_{32}^T\tilde{\boldsymbol{S}}\boldsymbol{M}_{32}+\boldsymbol{M}_{31}^T\tilde{\boldsymbol{Q}}\boldsymbol{M}_{31}-\boldsymbol{M}_{34}^T\tilde{\boldsymbol{Q}}\boldsymbol{M}_{34}\\&-(\tilde{\boldsymbol{X}}\boldsymbol{H}_2+\boldsymbol{H}_2^T\tilde{\boldsymbol{X}}^T)+\frac{h_2^2}{4}\boldsymbol{M}_{32}^T\boldsymbol{Q}_4\boldsymbol{M}_{32}+\frac{h_2^2}{4}\boldsymbol{M}_{33}^T\boldsymbol{Q}_6\boldsymbol{M}_{33}\\ \boldsymbol{\Sigma}_{32}=&\ 2\boldsymbol{M}_{32}^T\tilde{\boldsymbol{S}}\boldsymbol{M}_{33}+\boldsymbol{M}_{33}^T\tilde{\boldsymbol{R}}\boldsymbol{M}_{33},\\ \boldsymbol{\Sigma}_{33}=&\ \tilde{\boldsymbol{X}}\bar{\boldsymbol{R}}'\tilde{\boldsymbol{X}}^T+\boldsymbol{M}_{31}^T\boldsymbol{Q}_2\boldsymbol{M}_{31}\\ \nu=&\ h_2f_1^2\lambda_{\max}(\boldsymbol{Q}_1)+\frac{h_2^2}{4}f_1^2\lambda_{\max}(\boldsymbol{Q}_3)+\frac{h_2^2}{4}f_1^2\lambda_{\max}(\boldsymbol{Q}_5)\\&+\frac{h_2^3}{8}f_1^2\lambda_{\max}(\boldsymbol{E}_{fi}^T\tilde{\boldsymbol{R}}\boldsymbol{E}_{fi})\end{aligned}$$

If $\boldsymbol{\Sigma}_{31}+(h_2-\tau_2(t))\boldsymbol{\Sigma}_{32}+\tau_2(t)\boldsymbol{\Sigma}_{33}<0$, then $\dot{V}_2(t)\leq-\varepsilon\left\|\psi_3(t)\right\|^2+\nu$, where

$$\varepsilon=\lambda_{\min}\{-[\boldsymbol{\Sigma}_{31}+(h_2-\tau_2(t))\boldsymbol{\Sigma}_{32}+\tau_2(t)\boldsymbol{\Sigma}_{33}]\}.$$

Therefore, when $-\varepsilon\left\|\psi_3(t)\right\|^2+\nu<0$ and $\left\|\psi_3(t)\right\|^2>\frac{\nu}{\varepsilon}$, then $\dot{V}_2(t)<0$ is true. When $\psi_3(t)$ converges to the set $\nabla=\left\{\psi_3(t)\,\middle|\,\left\|\psi_3(t)\right\|^2\leq\frac{\nu}{\varepsilon}\right\}$, the system in Eq.(23) is uniformly eventually bounded.

The necessary and sufficient condition for the inequality $\boldsymbol{\Sigma}_{31}+(h_2-\tau_2(t))\boldsymbol{\Sigma}_{32}+\tau_2(t)\boldsymbol{\Sigma}_{33}<0$ to be valid are:

$$\boldsymbol{\Sigma}_{31}+h_2\boldsymbol{\Sigma}_{32}<0,\ \boldsymbol{\Sigma}_{31}+h_2\boldsymbol{\Sigma}_{33}<0\tag{38}$$

Under the zero initial condition, when $e_x(j_{k_3}) \neq 0$, $e_f(j_{k_3}) \neq 0$, the H_∞ performance index function is as follows:

$$\begin{aligned} J_2 = &\dot{V}_2(t) + x^T(t)x(t) - \gamma_2^2(e_x^{\mathrm{T}}(j_{k_3})e_x(j_{k_3}) \\ &+ e_f^{\mathrm{T}}(j_{k_3})e_f(j_{k_3}) + w^T(t)w(t) + e^T(i_{k_1})\boldsymbol{\Phi}e(i_{k_1}) \\ &- e^T(i_{k_1})\boldsymbol{\Phi}e(i_{k_1})) \end{aligned} \tag{39}$$

According to event trigger condition in Eq. (3), when $t \in [t_{k_2}, t_{k_2+1})$, the following inequality exists:

$$e^T(i_{k_1})\boldsymbol{\Phi}e(i_{k_1}) \leq \sigma_s\hat{x}^T(t_{k_2})\boldsymbol{\Phi}\hat{x}(t_{k_2}) \tag{40}$$

Let

$$\psi_4(t) = [x(t); x(j_{k_3}); \frac{1}{\tau_2(t)}\tilde{\boldsymbol{\Omega}}_0^T; \frac{1}{\tau_2(t)}\tilde{\boldsymbol{\Omega}}_1^T; e_x(j_{k_3}); e_f(j_{k_3}); w(t); \hat{x}(t_{k_2}); e(i_{k_1})]$$

where $\tilde{\boldsymbol{\Omega}}_0$, $\tilde{\boldsymbol{\Omega}}_1$ are similar to in Eq. (31),

$$\begin{aligned}
\boldsymbol{M}_{41} &= [\boldsymbol{I} \quad 0 \quad 0 \quad 0 \quad 0 \quad 0 \quad 0 \quad 0 \quad 0] \\
\boldsymbol{M}_{42} &= [\boldsymbol{I} \quad -\boldsymbol{I} \quad 0 \quad 0 \quad 0 \quad 0 \quad 0 \quad 0 \quad 0] \\
\boldsymbol{M}_{43} &= [\boldsymbol{A}_i \quad \boldsymbol{B}_i\boldsymbol{K}_j \quad 0 \quad 0 \quad \boldsymbol{B}_i\boldsymbol{K}_j \quad -\boldsymbol{E}_{fi} \quad \boldsymbol{E}_{wi} \quad 0 \quad 0] \\
\boldsymbol{M}_{44} &= [0 \quad \boldsymbol{I} \quad 0 \quad 0 \quad 0 \quad 0 \quad 0 \quad 0 \quad 0] \\
\boldsymbol{M}_{45} &= \begin{bmatrix} \boldsymbol{I} & 0 & 0 & 0 & 0 & 0 & 0 & 0 & 0 \\ 0 & \boldsymbol{I} & 0 & 0 & 0 & 0 & 0 & 0 & 0 \\ 0 & 0 & \boldsymbol{I} & 0 & 0 & 0 & 0 & 0 & 0 \\ 0 & 0 & 0 & \boldsymbol{I} & 0 & 0 & 0 & 0 & 0 \end{bmatrix} \\
\boldsymbol{M}_{46} &= \begin{bmatrix} 0 & 0 & 0 & 0 & \boldsymbol{I} & 0 & 0 & 0 & 0 \\ 0 & 0 & 0 & 0 & 0 & \boldsymbol{I} & 0 & 0 & 0 \\ 0 & 0 & 0 & 0 & 0 & 0 & \boldsymbol{I} & 0 & 0 \end{bmatrix} \\
\boldsymbol{M}_{47} &= [0 \quad 0 \quad 0 \quad 0 \quad 0 \quad 0 \quad 0 \quad \boldsymbol{I} \quad 0] \\
\boldsymbol{M}_{48} &= [0 \quad 0 \quad 0 \quad 0 \quad 0 \quad 0 \quad 0 \quad 0 \quad \boldsymbol{I}]
\end{aligned}$$

Then,

$$\begin{aligned}
&x(t) = \boldsymbol{M}_{41}\psi_4(t), \quad \varphi_2(t) = \boldsymbol{M}_{42}\psi_4(t) \\
&\dot{x}(t) = \boldsymbol{M}_{43}\psi_4(t) + \tau_2(t)\boldsymbol{E}_{fi}\dot{f}(t) \\
&x(j_{k_3}) = \boldsymbol{M}_{44}\psi_4(t), \quad e(i_{k_1}) = \boldsymbol{M}_{48}\psi_4(t) \\
&\hat{x}(t_{k_2}) = \boldsymbol{M}_{47}\psi_4(t), \quad \psi_3(t) = \boldsymbol{M}_{45}\psi_4(t) \\
&\begin{bmatrix} e_x^T(j_{k_3}) & e_f^T(j_{k_3}) & w^T(t) \end{bmatrix}^T = \boldsymbol{M}_{46}\psi_4(t)
\end{aligned}$$

Therefore, by combining (39) and (40), the following inequality can be derived,

$$J_2 \leq \psi_4^T(t)\left[\boldsymbol{\Sigma}_{41} + (h_2 - \tau_2(t))\boldsymbol{\Sigma}_{42} + \tau_2(t)\boldsymbol{\Sigma}_{43}\right]\psi_4(t) + \kappa \tag{41}$$

where

$$\begin{aligned}
\boldsymbol{\Sigma}_{41} = &\, 2\boldsymbol{M}_{41}^T\tilde{\boldsymbol{P}}\boldsymbol{M}_{43} + \boldsymbol{M}_{41}^T\tilde{\boldsymbol{Q}}\boldsymbol{M}_{41} - \boldsymbol{M}_{44}^T\tilde{\boldsymbol{Q}}\boldsymbol{M}_{44} - \boldsymbol{M}_{42}^T\tilde{\boldsymbol{S}}\boldsymbol{M}_{42} \\
&- \boldsymbol{M}_{45}^T(\tilde{\boldsymbol{X}}\boldsymbol{H}_2 + \boldsymbol{H}_2^T\tilde{\boldsymbol{X}}^T)\boldsymbol{M}_{45} + \boldsymbol{M}_{41}^T\boldsymbol{M}_{41} \\
&+ \frac{h_2^2}{4}\boldsymbol{M}_{43}^T\boldsymbol{Q}_6\boldsymbol{M}_{43} \\
&+ \sigma_s\boldsymbol{M}_{47}^T\boldsymbol{\Phi}\boldsymbol{M}_{47} - \boldsymbol{M}_{48}^T\boldsymbol{\Phi}\boldsymbol{M}_{48} + \frac{h_2^2}{4}\boldsymbol{M}_{42}^T\boldsymbol{Q}_4\boldsymbol{M}_{42} \\
&- \gamma_2^2\boldsymbol{M}_{46}^T\boldsymbol{M}_{46}
\end{aligned}$$

$$\begin{aligned}
\boldsymbol{\Sigma}_{42} &= 2\boldsymbol{M}_{42}^T\boldsymbol{S}'\boldsymbol{M}_{43} + \boldsymbol{M}_{43}^T\boldsymbol{R}'\boldsymbol{M}_{43} \\
\boldsymbol{\Sigma}_{43} &= \boldsymbol{M}_{45}^T\tilde{\boldsymbol{X}}\tilde{\tilde{\boldsymbol{R}}}\tilde{\boldsymbol{X}}^T\boldsymbol{M}_{45} + \boldsymbol{M}_{41}^T\boldsymbol{Q}_2\boldsymbol{M}_{41}
\end{aligned}$$

Similarly, when $\psi_4(t)$ finally converges to the set $\Delta' = \{\psi_4(t) \,|\, \|\psi_4(t)\|^2 \leq \frac{\nu}{\varepsilon'}\}$, the system in Eq. (23) is eventually uniformly bounded.

From the linear convex lemma, we obtain that $J_2 < \boldsymbol{0}$ is equivalent to the following inequalities:

$$\boldsymbol{\Sigma}_{41} + h_2\boldsymbol{\Sigma}_{42} < \boldsymbol{0}, \quad \boldsymbol{\Sigma}_{42} + h_2\boldsymbol{\Sigma}_{43} < \boldsymbol{0} \tag{42}$$

Let $\tilde{\boldsymbol{S}} = n_1\tilde{\boldsymbol{P}}, \tilde{\boldsymbol{R}} = n_2\tilde{\boldsymbol{P}}, \tilde{\boldsymbol{Q}} = n_3\tilde{\boldsymbol{P}}, \boldsymbol{Q}_2 = m_1\tilde{\boldsymbol{P}}, \boldsymbol{Q}_4 = m_2\tilde{\boldsymbol{P}}$, $\boldsymbol{Q}_6 = m_3\tilde{\boldsymbol{P}}$ and $\boldsymbol{K}_{1j} = \tilde{\boldsymbol{P}}\boldsymbol{B}_i\boldsymbol{K}_j$. We can turn the nonlinear matrix inequalities in Eq. (38) and (42) into linear matrix inequalities. By expanding Eq. (38) and (42) and applying the Schur complementary lemma, the Eq. (24), (25), (26) and (27) can be obtained, respectively.

The Eq. (41) is integrated from 0 to $+\infty$, then the following inequality can be obtained.

$$\begin{aligned}
&V_2(+\infty) - V_2(0) \\
&\leq -\int_0^{+\infty} x^T(s)x(s)ds + \gamma_2^2\int_0^{+\infty} w^T(s)w(s)ds \\
&+ \gamma_2^2\sum_{k=0}^{+\infty}(j_{k_3+1} - j_{k_3})[e_x^T(j_{k_3})e_x(j_{k_3}) + e_f^T(j_{k_3})e_f(j_{k_3})]
\end{aligned} \tag{43}$$

where $V_2(0) = 0$ and $V_2(+\infty) \geq 0$.

So, under zero initial condition, the inequality

$$\|x(t)\|_2^2 \leq \gamma_2^2[\|w(t)\|_2^2 + \sum_{k=0}^{+\infty}(j_{k_3+1} - t_{k_2})(\left\|e_x(j_{k_3})\right\|_2^2 + \left\|e_f(j_{k_3})\right\|_2^2)]$$

is true, then the proof is completed.

V. SIMULATION EXPERIMENT AND EXPERIMENT RESULTS ANALYSIS

To verify the feasibility and effectiveness of the theoretical results, the classical quadruple-tank model [37] was introduced. The schematic diagram of quadruple-tank model is shown in Figure 3.

In this simulation, x_1, x_2, x_3, x_4 represent the water level variations in each of the four tanks, and y_1, y_2, y_3, y_4 indicate the observations of the variation, respectively. The inputs u_1 and u_2 are the voltage values to the two pumps that provide water to the four tanks.

The fuzzy membership function was assumed to be $M_1(x_4) = sin^2x_4$, $M_2(x_4) = cos^2x_4$, $M_3(x_4) = sin^2x_4$, $M_4(x_4) = cos^2x_4$, and the nonlinear system is expressed as a T-S fuzzy system with four rules.

Rule i: if x_4 is M_i, $i = 1, 2, 3, 4$, then

$$\begin{cases} \dot{x}(t) = \boldsymbol{A}_ix(t) + \boldsymbol{B}_iu(t) + \boldsymbol{E}_{fi}f(t) + \boldsymbol{E}_{wi}w(t) \\ y(i_{k_1}) = \boldsymbol{C}_ix(i_{k_1}) + \boldsymbol{E}_{vi}v(i_{k_1}) \end{cases}$$

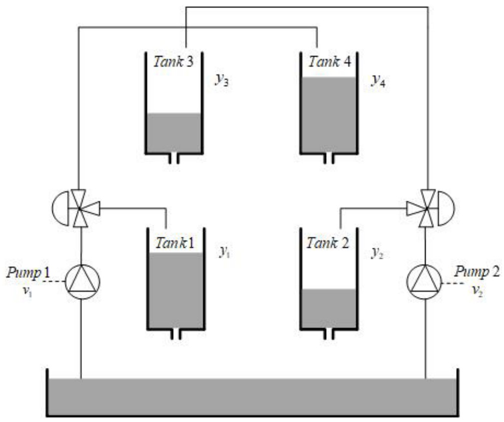

FIGURE 3. Schematic diagram of the quadruple-tank model.

$$A_1 = \begin{bmatrix} -0.016 & 0 & 0.042 & 0 \\ 0 & -0.011 & 0 & 0.033 \\ 0 & 0 & -0.042 & 0 \\ 0 & 0 & 0 & -0.033 \end{bmatrix},$$
$$A_2 = \begin{bmatrix} -0.022 & 0 & 0.061 & 0 \\ 0 & -0.018 & 0 & 0.049 \\ 0 & 0 & -0.064 & 0 \\ 0 & 0 & 0 & -0.049 \end{bmatrix},$$
$$A_3 = \begin{bmatrix} -0.031 & 0 & 0.053 & 0 \\ 0 & -0.021 & 0 & 0.067 \\ 0 & 0 & -0.083 & 0 \\ 0 & 0 & 0 & -0.061 \end{bmatrix},$$
$$A_4 = \begin{bmatrix} -0.039 & 0 & 0.106 & 0 \\ 0 & -0.0276 & 0 & 0.0826 \\ 0 & 0 & -0.107 & 0 \\ 0 & 0 & 0 & -0.0827 \end{bmatrix},$$
$$B_1 = \begin{bmatrix} 0.083 & 0 \\ 0 & 0.063 \\ 0 & 0.048 \\ 0.031 & 0 \end{bmatrix}, \quad B_2 = \begin{bmatrix} 0.1246 & 0 \\ 0 & 0.093 \\ 0 & 0.071 \\ 0.045 & 0 \end{bmatrix},$$
$$B_3 = \begin{bmatrix} 0.165 & 0 \\ 0 & 0.125 \\ 0 & 0.097 \\ 0.063 & 0 \end{bmatrix}, \quad B_4 = \begin{bmatrix} 0.2076 & 0 \\ 0 & 0.1576 \\ 0 & 0.13 \\ 0.0776 & 0 \end{bmatrix},$$
$$E_{\omega 1} = \begin{bmatrix} 0.01 \\ 0.01 \\ 0 \\ 0.01 \end{bmatrix}, \quad E_{\omega 2} = \begin{bmatrix} 0.016 \\ 0.016 \\ 0 \\ 0.016 \end{bmatrix}, \quad E_{\omega 3} = \begin{bmatrix} 0.02 \\ 0.02 \\ 0 \\ 0.02 \end{bmatrix},$$
$$E_{\omega 4} = \begin{bmatrix} 0.024 \\ 0.024 \\ 0 \\ 0.024 \end{bmatrix}, \quad E_{f1} = -\begin{bmatrix} 0.083 & 0 & 0 & 0.031 \end{bmatrix}^T,$$
$$E_{f2} = -\begin{bmatrix} 0.1246 & 0 & 0 & 0.0464 \end{bmatrix}^T,$$
$$E_{f3} = -\begin{bmatrix} 0.167 & 0 & 0 & 0.061 \end{bmatrix}^T,$$
$$E_{f4} = -\begin{bmatrix} 0.2076 & 0 & 0 & 0.0774 \end{bmatrix}^T,$$
$$C_1 = diag\{0.5 \quad 0.5 \quad 0.5 \quad 0.5\},$$
$$C_2 = diag\{0.48 \quad 0.48 \quad 0.48 \quad 0.48\},$$
$$C_3 = diag\{0.46 \quad 0.46 \quad 0.46 \quad 0.46\},$$
$$C_4 = diag\{0.52 \quad 0.52 \quad 0.52 \quad 0.52\},$$
$$E_{v1} = \begin{bmatrix} 0.015 & 0 & 0.015 & 0.015 \end{bmatrix}^T,$$
$$E_{v2} = \begin{bmatrix} 0.0224 & 0 & 0.0224 & 0.0224 \end{bmatrix}^T,$$
$$E_{v3} = \begin{bmatrix} 0.030 & 0 & 0.025 & 0.027 \end{bmatrix}^T,$$
$$E_{v4} = \begin{bmatrix} 0.0374 & 0 & 0.031 & 0.0326 \end{bmatrix}^T, \quad \text{and}$$
$$f(t) = \begin{cases} 0 & t \le 100 \\ 2 + 2sin0.01\pi(t-100) & 100 < t \le 800, \end{cases}$$

where the disturbance $w(t)$ and the noise $v(i_{k_1})$ are the independent white noise process that obey $N(0.1, 0.01)$, the initial state is $x(0) = [4 \quad 4 \quad 2 \quad 2]^T$ and the sampling period $h = 0.1s$.

Let $n_1 = 0.1$, $n_2 = 8$, $n_3 = 3$, $\gamma_1 = 2.6458$, the observer gain matrix L_j and fault estimation gain matrix F_j can be obtained through the Theorem 1.

$$L_1 = \begin{bmatrix} 8.2899 & -0.0021 & 0.0379 & -0.1277 \\ -0.0007 & 8.6201 & 0.0000 & 0.0170 \\ 0.0014 & 0.0000 & 8.6078 & 0.0029 \\ -0.1282 & -0.0108 & 0.0036 & 8.5643 \end{bmatrix}$$
$$L_2 = \begin{bmatrix} 8.8421 & -0.0023 & 0.0242 & -0.0568 \\ -0.0011 & 8.9803 & -0.0001 & 0.0231 \\ -0.0326 & -0.0001 & 8.9658 & -0.0093 \\ -0.0567 & -0.0195 & -0.0078 & 8.9500 \end{bmatrix}$$
$$L_3 = \begin{bmatrix} 9.2159 & -0.0033 & 0.0125 & -0.0642 \\ -0.0015 & 9.3711 & -0.0001 & 0.0305 \\ -0.0343 & -0.0001 & 9.3556 & -0.0137 \\ -0.0687 & -0.0304 & -0.0140 & 9.3358 \end{bmatrix}$$
$$L_4 = \begin{bmatrix} 8.1357 & -0.0038 & 0.0251 & -0.0669 \\ -0.0017 & 8.2913 & -0.0002 & 0.0319 \\ -0.0646 & -0.0001 & 8.2770 & -0.0163 \\ -0.0664 & -0.0346 & -0.0145 & 8.2586 \end{bmatrix}$$
$$F_1 = \begin{bmatrix} -18.8634 & -0.0615 & -0.0393 & -6.9835 \end{bmatrix}$$
$$F_2 = \begin{bmatrix} -19.2139 & -0.0529 & 0.0054 & -7.1159 \end{bmatrix}$$
$$F_3 = \begin{bmatrix} -19.3179 & -0.0414 & 0.0353 & -7.1636 \end{bmatrix}$$
$$F_4 = \begin{bmatrix} -16.4676 & -0.0252 & 0.0513 & -6.1005 \end{bmatrix}$$

Set $n_1 = 3.1$, $n_2 = 0.1$, $n_3 = 3$, $m_1 = m_2 = m_3 = 0.2$, $\sigma_s = 0.01$, $\gamma_2 = 3.1623$, $h_{t_k}^{\max} = 0.2s$, $\tau_M^{DoS} = 2$ in Theorem 2, then the maximum time delay upper bound $h_2 = h_{t_k}^{\max} + \tau_M^{DoS} h_{t_k}^{\max} = 0.6s$.

According to $\left(I - B_i B_j^+\right) E_{fi} = 0$, we can obtain the fault adjustment matrices B_j^+ as follows.

$$B_1^+ = \begin{bmatrix} 11.9550 & -10.5732 & 0 & 0.2496 \\ 0 & 0 & 0 & 0 \end{bmatrix}$$
$$B_2^+ = \begin{bmatrix} 7.9945 & -7.0997 & 0 & 0.1612 \\ 0 & 0 & 0 & 0 \end{bmatrix}$$
$$B_3^+ = \begin{bmatrix} 5.9824 & -5.2895 & 0 & 0.1226 \\ 0 & 0 & 0 & 0 \end{bmatrix}$$

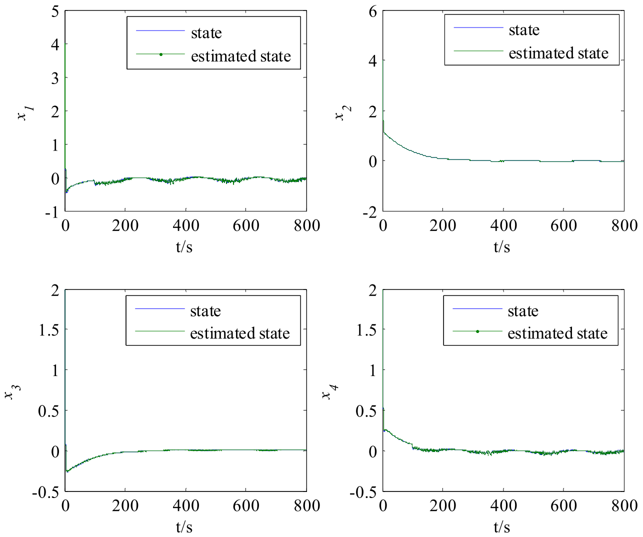

FIGURE 4. States and their estimations with DoS attack.

$$B_4^+ = \begin{bmatrix} 4.7783 & -4.2264 & 0 & 0.0995 \\ 0 & 0 & 0 & 0 \end{bmatrix}$$

Then, the event trigger weight matrix $\mathbf{\Phi}$ and the state feedback gain matrix $\boldsymbol{K}_j$ can be obtained cooperatively through Theorem 2.

$$\mathbf{\Phi} = 10^8 \times \begin{bmatrix} 0.1874 & 0 & 0 & 0 \\ 0 & 0.1874 & 0 & 0 \\ 0 & 0 & 0.1874 & 0 \\ 0 & 0 & 0 & 0.1874 \end{bmatrix}$$

$$\boldsymbol{K}_1 = \begin{bmatrix} -21.4008 & 0.3699 & -0.9239 & -25.9985 \\ 0.3722 & -9.4487 & -40.5598 & -2.4253 \end{bmatrix}$$

$$\boldsymbol{K}_2 = \begin{bmatrix} -14.5473 & 0.1054 & -0.5917 & -16.7667 \\ 0.1686 & -6.4157 & -26.9843 & -1.4539 \end{bmatrix}$$

$$\boldsymbol{K}_3 = \begin{bmatrix} -10.4781 & 0.2925 & -0.7056 & -13.1187 \\ 0.3238 & -4.5570 & -20.0038 & -1.4220 \end{bmatrix}$$

$$\boldsymbol{K}_4 = \begin{bmatrix} -8.4232 & 0.3520 & -0.6611 & -10.4357 \\ 0.2814 & -3.2303 & -15.3948 & -1.2080 \end{bmatrix}$$

A. STATE AND FAULT ESTIMATION

Random DoS attack was applied to the edge control network of the sensor-controller and controller-actuator, and the maximum number of consecutive packet loss is $\tau_M^{DoS} = 2$. Under DoS attack, the system state, estimation state, state estimation error, continuous time-varying fault and fault estimation error were obtained, as shown in Figures 4–7.

After adding the DoS attack, the state and estimated state appear to slightly fluctuate in Figure 4, and the state estimation error is almost zero in Figure 5, and the fault estimation follows the system fault closely in Figure 6, and the fault estimation error does not exceed ± 0.3 after 200s in Figure 7. Therefore, these results show that the designed observer in this paper can estimate fault accurately and timely under DoS attack; at the same time, it can prevent disturbance and tolerate attack.

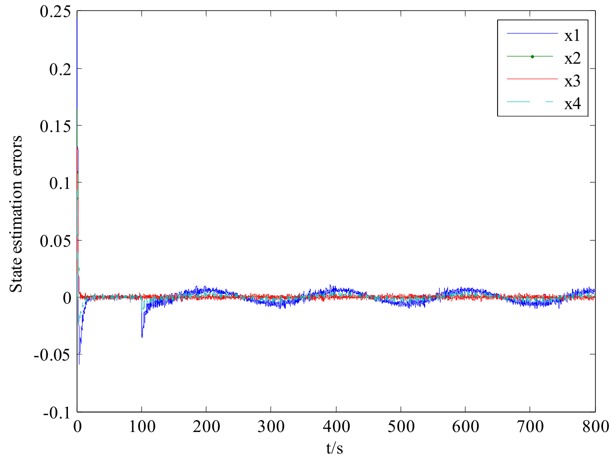

FIGURE 5. State estimation errors with DoS attack.

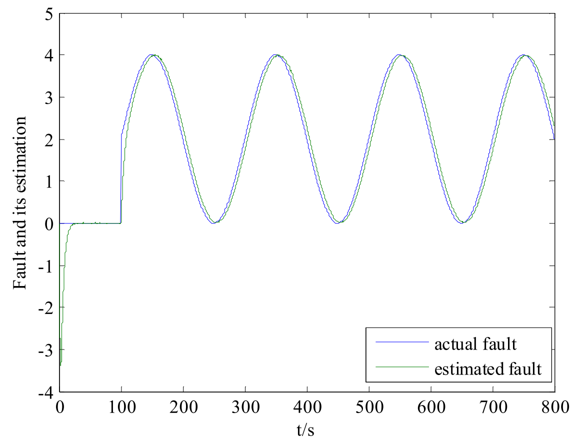

FIGURE 6. Continuous time-varying fault and its estimation with DoS attack.

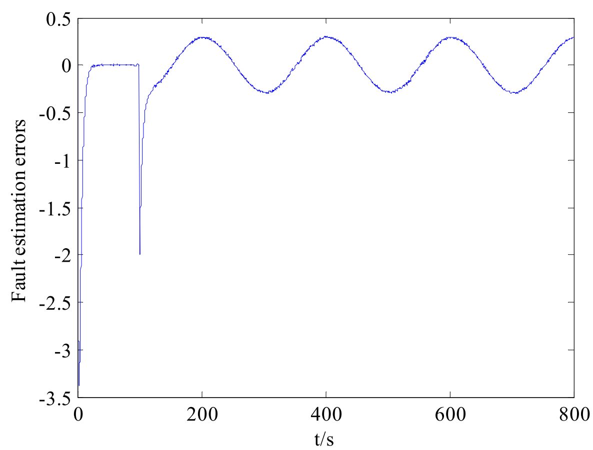

FIGURE 7. Fault estimation error with DoS attack.

B. CO-DESIGN OF SECURITY CONTROL AND COMMUNICATION FOR CPS

Under the limitation of γ_2, the maximum allowable delay upper bound $h_2^A = 2.3646s$ can be obtained by using the LMI toolbox. According to the equation $h_2^A = h_{t_{k_2}}^{\max} + \tau_M^{DoS} h_{t_{k_2}}^{\max}$,

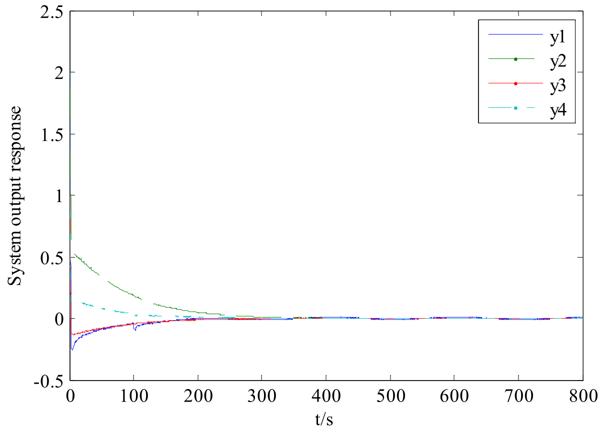

FIGURE 8. System output response curve with fault and without DoS attack.

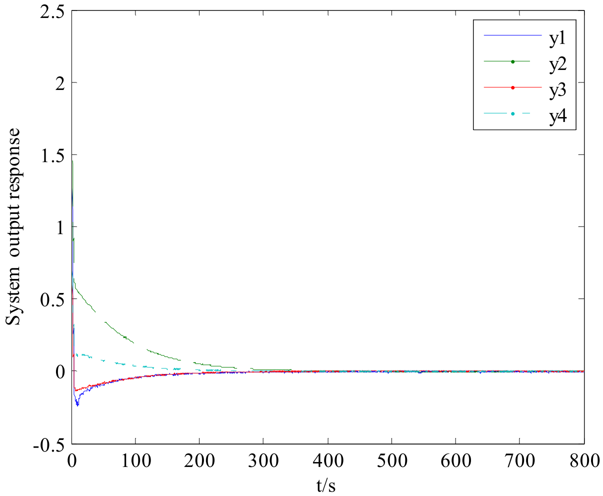

FIGURE 9. System output response curve with DoS attack and without fault $\tau_M^{DoS} = 2$.

let $h_{t_{k_2}}^{\max} = 0.2s$ and the simulation time is 800s, the actual maximum allowable consecutive packet loss is taken as $\tau_{MA}^{DoS} = 10$. Then, we discussed the following three cases.

Case I: There is a fault but no DoS attack

When the system with a fault and without DoS attack, the system output response curve is shown in Figure 8.

Case II: There is DoS attack but no fault

When the system with DoS attack and without fault, the maximum consecutive packet loss caused by the DoS attack is $\tau_M^{DoS} = 2$, $\tau_M^{DoS} = 9$ and $\tau_M^{DoS} = 13$, and the corresponding output response curve of the system are shown in Figure 9, 10 and 11.

Case III: There are both DoS attack and fault

When the system has both DoS attack and fault simultaneously, the maximum consecutive packet loss caused by the DoS attack respectively is $\tau_M^{DoS} = 2$, $\tau_M^{DoS} = 9$ and $\tau_M^{DoS} = 13$, and the corresponding output response curve of the system are shown in Figure 12, 13 and 14.

In Figure 8–14, the output response of the system with/without DoS attack and with/without fault are given. By comparison, it can be seen that:

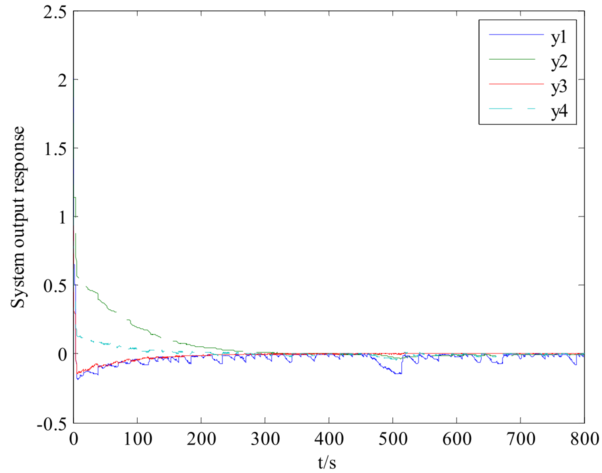

FIGURE 10. System output response curve with DoS attack and without fault $\tau_M^{DoS} = 9$.

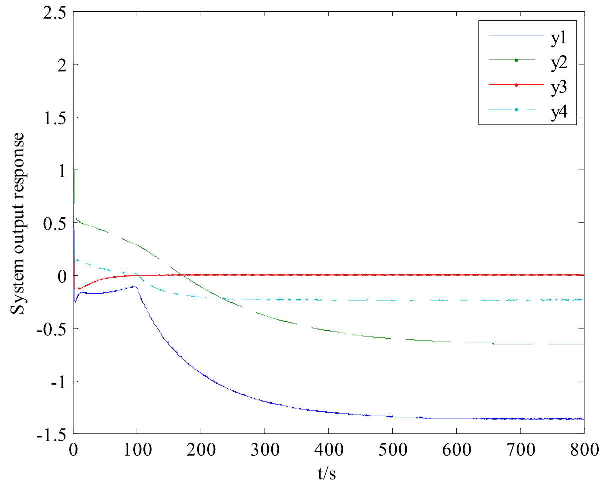

FIGURE 11. System output response curve with DoS attack and without fault $\tau_M^{DoS} = 13$.

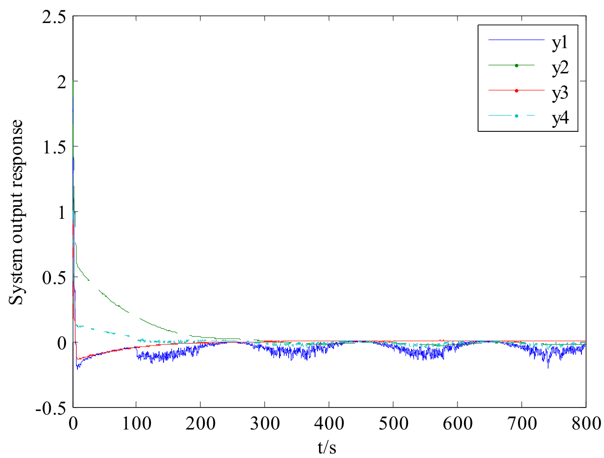

FIGURE 12. System output response curve with fault and DoS attack $\tau_M^{DoS} = 2$.

1) When the system has no DoS attack and only a time-varying fault, the system is not sensitive to fault at this time, which means that the method in this paper can actively tolerate fault.

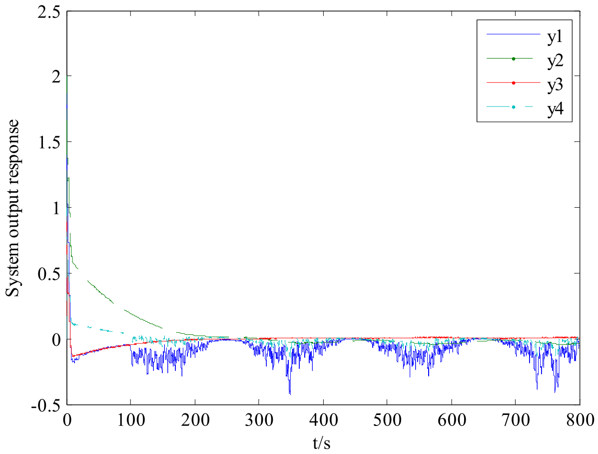

FIGURE 13. System output response curve with fault and DoS attack $\tau_M^{DoS} = 9$.

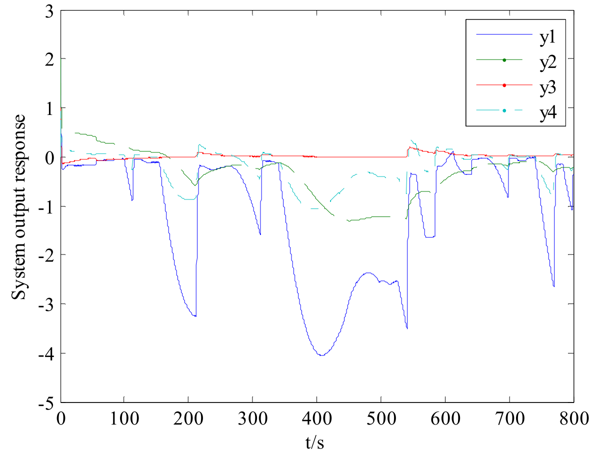

FIGURE 14. System output response curve with fault and DoS attack $\tau_M^{DoS} = 13$.

2) If there is only DoS attack but no fault in the system, with the increase of maximum consecutive packet loss τ_M^{DoS}, the stability of the system becomes worse.

3) If there are both DoS attack and time-varying fault, the system instability is aggravated. However, when the system's maximum consecutive packet loss is within the allowed range $\tau_{MA}^{DoS} = 10$, the system can remain stable and is not sensitive to DoS attack; that is, it has the dual security defence capability to tolerate fault actively and attack passively. Once the maximum number of consecutive packet loss is more than $\tau_{MA}^{DoS} = 10$, as shown in Figure 14, the system is unable to work normally. As the number of consecutive packet loss caused by DoS attack increases, the system will become unstable. This also fully demonstrates that using the proposed method in the paper, within the maximum allowable packet loss caused by DoS attack, the nonlinear CPS can effectively resist the impact of the fault, and be insensitive to the influence of the DoS attack. Therefore, the system has dual security capability.

In Figure 15, let $\tau_M^{DoS} = 2$ and $\sigma_s = 0.01$, in 800s simulation time. Compared with the 8000 transmitted data under the periodic time trigger scheme, there are 4,978 data

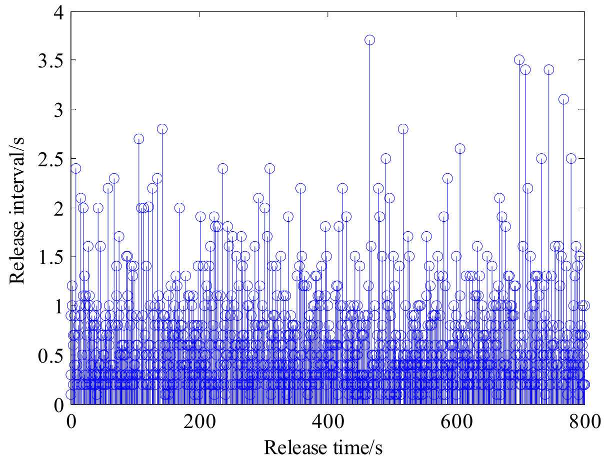

FIGURE 15. Release instants and release interval for non-uniform transmission CPS with DETCS.

transmitted to the side of ZOH under DoS attack based on DETCS, the number of the transmitted data is reduced by nearly half. This also indicates that the method in this paper not only can carry out dual security control for fault and DoS attack, but also effectively save network communication resources and improve system efficiency.

VI. CONCLUSION

Based on DETCS, the co-design method between dual security control and communication with actuator fault and DoS attack for nonlinear CPS was studied. First, combining with the idea of edge computing, the computing task was partially migrated to the edge device, and a nonlinear CPS closed-loop model was established that integrates actuator fault, DoS attack and discrete event triggering conditions. Second, using less conservative techniques such as affine Bessel-Legendre inequality, a robust observer for state and fault estimation and the co-design method of the dual security control and communication with actuator fault and DoS attack were given. Finally, the simulation results further show that the proposed method not only has the ability of dual security control, but also can accurately estimate system fault and state in real time, and effectively save communication resources under the actuator fault and DoS attack. However, the processing method of DoS attack is passive in this paper, and how to deal with fault and attack, by constructing online attack detection mechanism in an active way, and improving the dual security control level of nonlinear CPS, will be the next research work.

REFERENCES

[1] H. Y. Li, M. H. Wei, J. Huang, B. H. Qiu, Y. Zhao, W. C. Luo, and X. He, "Survey on cyber-physical systems," *Acta Autom. Sin*, vol. 45, no. 1, pp. 37–50, Jan. 2019.

[2] R. Alguliyev, Y. Imamverdiyev, and L. Sukhostat, "Cyber-physical systems and their security issues," *Comput. Ind.*, vol. 100, pp. 212–223, Sep. 2018.

[3] R. Fu, X. Huang, Y. Xue, Y. Wu, Y. Tang, and D. Yue, "Security assessment for cyber physical distribution power system under intrusion attacks," *IEEE Access*, vol. 7, pp. 75615–75628, 2019.

[4] H. C. Cao and W. Li, "Non-fragile robust fault-tolerant control for uncertain NCS with actuator saturation," *Control Decis.*, vol. 28, no. 12, pp. 1874–1883, Dec. 2013.

[5] Y. J. Li and W. Li, "Co-design between α/H_∞ fault-tolerant control of networked control system and network communication," *J. Jilin Univ. (Eng. Technol. Ed.)*, vol. 46, no. 6, pp. 2010–2020, Jun. 2016.

[6] J. R. Fan and H. J. Fang, "Robust fault-tolerant control for networked control system with variable sampling period," *Control Eng.*, vol. 20, no. 5, pp. 859–863, May 2013.

[7] Y. Li, Z. Ma, and S. Tong, "Adaptive fuzzy output-constrained fault-tolerant control of nonlinear stochastic large-scale systems with actuator faults," *IEEE Trans. Cybern.*, vol. 47, no. 9, pp. 2362–2376, Sep. 2017.

[8] X. He, Z. Wang, L. Qin, and D. Zhou, "Active fault-tolerant control for an Internet-based networked three-tank system," *IEEE Trans. Control Syst. Technol.*, vol. 24, no. 6, pp. 2150–2157, Nov. 2016.

[9] Y. J. Li and W. Li, "Satisfactory integrated design between failure accommodation and communication for non-uniform transmission networked control system under discrete event-triggered communication scheme," *J. Jilin Univ. (Eng. Technol. Ed.)*, vol. 48, no. 1, pp. 245–258, Jan. 2018.

[10] A. B. Qiu, J. Zhang, B. Jiang, and J. P. Gu, "Event-triggered sampling and fault-tolerant control co-design based on fault diagnosis observer," *J. Syst. Eng. Electron.*, vol. 29, no. 1, pp. 176–186, Feb. 2018.

[11] F. Xu, J. Tan, X. Wang, V. Puig, B. Liang, and B. Yuan, "Mixed active/passive robust fault detection and isolation using set-theoretic unknown input observers," *IEEE Trans. Autom. Sci. Eng.*, vol. 15, no. 2, pp. 863–871, Apr. 2018.

[12] J. Wang, S. Z. Li, and W. Li, "Hybrid active-passive robust fault-tolerant control for a networked control system based on an event-triggered scheme," *J. Lanzhou Univ. Tech*, vol. 46, no. 2, pp. 144–152, Jun. 2017.

[13] J. Wang, X. W. Yao, and W. Li, "Hybrid fault-tolerant control method research of NNCS," *Control Decis.*, vol. 33, no. 2, pp. 316–329, Feb. 2018.

[14] D. Ye and S. P. Luo, "A co-design methodology for cyber-physical systems under actuator fault and cyber-attack," *J. Franklin Inst.*, vol. 356, no. 4, pp. 1856–1879, Mar. 2019.

[15] W. Li, Y. Shi, and Y. Li, "Research on secure control and communication for cyber-physical systems under cyber-attacks," *Trans. Inst. Meas. Control*, vol. 41, no. 12, pp. 3421–3437, Aug. 2019, doi: 10.1177/0142331219826658.

[16] P. Shakarian, "Stuxnet: Cyberwar revolution in military affairs," DTIC, Fort Belvoir, VA, USA, Tech. Rep., 2011.

[17] T. M. Chen, "Stuxnet, the real start of cyber warfare?" *IEEE Netw.*, vol. 24, no. 6, pp. 2–3, Nov./Dec. 2010.

[18] Y. Cherdantseva, P. Burnap, A. Blyth, P. Eden, K. Jones, and H. Soulsby, "A review of cybersecurity risk assessment methods for SCADA systems," *Comput. Secur.*, vol. 56, pp. 1–27, Feb. 2016.

[19] Y. Tang, Q. Chen, M. Y. Li, Q. Wang, M. Ni, and Y. Liang, "Overview on cyber-attacks against cyber-physical power system," *Autom. Electr. Power Syst.*, vol. 40, no. 17, pp. 59–69, Sep. 2016.

[20] T. Liu, J. Tian, and J. Z. Wang, "Integrated security threats and defence of cyber-physical systems," *Acta Autom. Sin.*, vol. 45, no. 1, pp. 5–24, Jan. 2019.

[21] S. Feng and P. Tesi, "Resilient control under denial-of-service: Robust design," *Automatica*, vol. 79, pp. 42–51, May 2017.

[22] C. De Persis and P. Tesi, "Input-to-state stabilizing control under denial-of-service," *IEEE Trans. Autom. Control*, vol. 60, no. 11, pp. 2930–2944, Nov. 2015.

[23] S. Hu, D. Yue, X. Xie, X. Chen, and X. Yin, "Resilient event-triggered controller synthesis of networked control systems under periodic dos jamming attacks," *IEEE Trans. Cybern.*, vol. 49, no. 12, pp. 4271–4281, Dec. 2019.

[24] M. Wang and B. Xu, "Observer-based guaranteed cost control of cyber-physical systems under DoS jamming attacks," *Eur. J. Control*, vol. 48, pp. 21–29, Jul. 2019.

[25] L. Su and D. Ye, "A cooperative detection and compensation mechanism against Denial-of-service attack for cyber-physical systems," *Inf. Sci.*, vol. 444, pp. 122–134, May 2018.

[26] W. Shi, H. Sun, J. Cao, Q. Zhang, and W. Liu, "Edge computing-an emerging computing model for the Internet of everything era," *J. Comput. Res. Develop.*, vol. 54, no. 5, pp. 907–924, May 2017.

[27] W. Shi, J. Cao, Q. Zhang, Y. Li, and L. Xu, "Edge computing: Vision and challenges," *IEEE Internet Things J.*, vol. 3, no. 5, pp. 637–646, Oct. 2016.

[28] V. S. Dolk, P. Tesi, C. De Persis, and W. P. M. H. Heemels, "Event-triggered control systems under denial-of-service attacks," *IEEE Trans. Control Netw. Syst.*, vol. 4, no. 1, pp. 93–105, Mar. 2017.

[29] C. Peng, Q.-L. Han, and D. Yue, "To transmit or not to transmit: A discrete event-triggered communication scheme for networked Takagi–Sugeno fuzzy systems," *IEEE Trans. Fuzzy Syst.*, vol. 21, no. 1, pp. 164–170, Feb. 2013.

[30] C. Peng and T. C. Yang, "Event-triggered communication and control co-design for networked control systems," *Automatica*, vol. 49, no. 5, pp. 1326–1332, May 2013.

[31] A.-Y. Lu and G.-H. Yang, "Event-triggered secure observer-based control for cyber-physical systems under adversarial attacks," *Inf. Sci.*, vol. 420, pp. 96–109, Dec. 2017.

[32] H. Q. Xiao, Y. He, and M. Wu, "H_∞ output tracking control for sampled-data networked control systems in T-S fuzzy model," *Acta Autom, Sin.*, vol. 41, no. 3, pp. 661–668, Mar. 2015.

[33] E. Fridman, "A refined input delay approach to sampled-data control," *Automatica*, vol. 46, no. 2, pp. 421–427, Feb. 2010.

[34] A. B. Qiu, H. G. Ji, and J. P. Gu, "Optimal integrated design of time-varying fault estimation and accommodation for non-uniform sampled data systems," *Acta Autom. Sin*, vol. 40, no. 7, pp. 1493–1504, Jul. 2014.

[35] A. Seuret and F. Gouaisbaut, "Stability of linear systems with time-varying delays using Bessel–Legendre inequalities," *IEEE Trans. Autom. Control*, vol. 63, no. 1, pp. 225–232, Jan. 2018.

[36] W. I. Lee, S. Y. Lee, and P. Park, "Affine Bessel–Legendre inequality: Application to stability analysis for systems with time-varying delays," *Automatica*, vol. 93, pp. 535–539, Jul. 2018.

[37] K. Johansson, "The quadruple-tank process: A multivariable laboratory process with an adjustable zero," *IEEE Trans. Control Syst. Technol.*, vol. 8, no. 3, pp. 456–465, May 2000.

LI ZHAO was born in Qingyang, Gansu, China, in 1987. She received the B.S. and M.S. degrees from the Lanzhou University of Technology, in 2011 and 2014, respectively. She is currently pursuing the Ph.D. degree with the College of Electrical and Information Engineering, Lanzhou University of Technology. She is mainly engaged in fault tolerance and attack tolerance for CPS.

WEI LI was born in Xi'an, Shanxi, China, in 1963. She is currently a Professor and a Ph.D. Candidate Tutor with the College of Electrical and Information Engineering, Lanzhou University of Technology. Her research interests include fault diagnosis, fault-tolerant control, and attack tolerance control.